Comparison of the effect of mix proportion parameters on behaviour of geopolymer and Portland cement mortars

Kwasny, J., Soutsos, M. N., McIntosh, J. A., & Cleland, D. J. (2018). Comparison of the effect of mix proportion parameters on behaviour of geopolymer and Portland cement mortars. *Construction and Building Materials*, *187*, 635-651. https://doi.org/10.1016/j.conbuildmat.2018.07.165

Published in:
Construction and Building Materials

Document Version:
Peer reviewed version

Comparison of the effect of mix proportion parameters on behaviour of geopolymer and Portland cement mortars

Jacek Kwasny[a,1*], Marios N. Soutsos[a,2], John A. McIntosh[a,b,3], and David J. Cleland[a,4]

[a] School of Natural and Built Environment, Queen's University Belfast,
Belfast BT9 5AG, UK

[b] banah UK Ltd, 1b Letterloan Road, Macosquin, Coleraine BT51 4PP, Northern Ireland, UK

[1] j.kwasny@qub.ac.uk (* corresponding author)

[2] m.soutsos@qub.ac.uk

[3] andrew@banahuk.co.uk

[4] d.cleland@qub.ac.uk

ABSTRACT

This work focuses on low-purity kaolin, widely accessible throughout the globe. Room temperature cured geopolymer mortars (GPMs) were formulated using an aluminosilicate precursor based on calcined lithomarge and potassium silicate activator. The effect of mix proportion parameters on the engineering properties of GPMs was investigated. The behaviour of GPMs was compared with that of Portland cement-based mortars (PCMs). Statistically designed experiments revealed that an increase in water-to-solid (w/s) ratio had *a dominant effect on increasing the workability and setting time while decreasing the compressive strength of GPMs. In contrast to PCMs, GPMs proportioned with a constant water content showed a non-linear relationship between the w/s ratio and workability, which could be associated with changes to paste/sand proportions and/or water/alkali proportions. Like-for-like comparison of GPMs and PCMs showed that GPMs require lower free water content, and can offer shorter setting times and a rapid strength development.*

Keywords: Kaolin; Lithomarge; Geopolymer mortars; Portland cement mortars; Centre composite design; Workability; Setting time; Compressive strength;

1 INTRODUCTION

Geopolymer-based concretes are a new class of construction materials, where the cementitious binder is replaced with geopolymer alternatives, typically of low carbon footprint. Geopolymer binders are produced by reacting an alumino-silicate precursor, often a waste or a by-product material, with an alkali-silicate solution, also called chemical activator [1]. An inorganic polymerisation reaction results in the formation of hardened material with a three-dimensional and amorphous microstructure. Thanks to the unique, ceramic-like microstructure, geopolymer-based materials have been reported to have potentially equivalent, or even superior, physical and durability properties when compared to conventional materials made with Portland cement [2]. Geopolymers are most frequently renowned for a fast rate of strength development, fast setting time, resistance to chemical attack and improved fire resistance [3]. However, where the concrete/construction industry is concerned, geopolymer concrete still has to be proven to be more user-friendly and cost-effective, and to comply with specific engineering properties in order to gain more popularity.

Various alumino-silicate source types can be used as precursors for geopolymerisation. Among the most common are metakaolin (*i.e.* high purity kaolin) [4, 5] and different types of calcined clays [6-9], slags [2, 10, 11] and ashes [2, 12-14]. However, due to geographical or industrial diversity across the globe, precursors containing metakaolin or some industrial by-products (such as fly ash or ground granulated blast furnace slag) may not be locally available. Economy and sustainability of geopolymer technology are hindered by the need to source the precursor elsewhere and transport it to the place of further processing or intended use. Therefore, it is important to investigate the possibility of using locally available, naturally occurring, low purity materials, such as clays. These clays, being abandoned by industry, have the advantage of being cheaper than the high purity alternatives (*e.g.* metakaolin) or materials which are difficult/expensive to get access to. It has been recently shown that low purity kaolinitic clays can be calcined and used to produce geopolymer binders with compressive strengths exceeding 50 MPa [15-21].

Large deposits of kaolin-containing soft rock, called lithomarge, exist in Northern Ireland as part of the Interbasaltic Formation (IBF) [22]. Cooper [23] reported that lithomarge primarily contains kaolinite ($Al_2Si_2O_5(OH)_4$), gibbsite ($Al(OH)_3$), goethite ($FeO(OH)$), hematite (Fe_2O_3) and various smectite minerals. IBF material is typically seen as a nuisance by quarry owners. However, because of its kaolinite content, IBF could be used as an aluminosilicate source for the commercially viable formation of geopolymer binders, hence providing a large resource for future commercial production. Since the mineralogy of lithomarge varies, it is important to have an appropriate methodology in place to be able to identify the most appropriate precursor material for the production of geopolymer binder. McIntosh *et al.* [19] developed a protocol, not geographically limited to Northern Ireland, for refining the selection process of lithomarge suitable for calcination. It was shown that to produce binders with minimum compressive strength of 50 MPa, the kaolinite content should exceed 60% by weight of the original rock [19].

After decades of research evidence, it has been well established that the water-to-cement (w/c) ratio (or water-to-binder ratio for concrete made with additions, also called supplementary cementitious materials) is the dominant factor influencing most properties of conventional Portland cement-based concrete [24]. For a given set of concrete ingredients, selection of the w/c ratio and binder content are required at the mix design stage to produce concretes that meet specific strength and durability requirements. On the other hand, to achieve a desired workability at a given w/c ratio, a suitable content of free water in the mix or, more specifically, a suitable content of paste filling spaces between the aggregate particles, is needed. In the upcoming years, geopolymer binder concretes formulated using low purity kaolinitic clays will likely gain wider construction market access. Therefore, it is of importance to understand their behavior and compare it to that of conventional concretes. Recognising these needs, the overall aim of this work was to characterise the behaviour of lithomarge-based geopolymer mortars (GPMs), paving the way for the future development of a mix design of geopolymer concrete. GPM mixes were compared to Portland cement mortars (PCMs) to demonstrate whether the GPMs can be used by the industry in a similar way to a Portland cement system. Therefore, the primary objective of this research was to assess the effect of mix proportion parameters, *i.e.* water-to-solid (w/s) ratio, paste volume and free water content, on workability, setting times and compressive strengths of room temperature cured geopolymer mortars formulated using an aluminosilicate precursor based on calcined lithomarge and a potassium silicate activator. Design of experiments approach (DoE) was used to simultaneously investigate the effect of w/s ratio and paste volume on the properties of GPMs. In addition, the effect of a wide range of w/s ratios was studied on GPM mixes made with either fixed paste volume (varied free water content) or with a fixed free water content (varied paste volume). The behaviour of these two groups of GPM mixes was compared with that of Portland cement counterparts made with varied w/c ratios. The secondary objective was to directly compare the performance of selected GPMs with that of Portland cement alternatives in the same strength class (normal and high strength) and formulated with the same paste volume.

2 RESEARCH SIGNIFICANCE

In recent years there has been tremendous research effort into development and characterisation of cement free binders and concretes, to overcome shortcomings and lower the overall environmental impact of Portland cement concrete. However, most of the effort has been dedicated towards usage of slags, ashes or pure metakaolin. This paper provides data regarding the effect of variation in selected mix proportion parameters (w/s ratio, paste volume and free water content) on workability, setting time and compressive strength of geopolymer mortars formulated with a lithomarge based precursor, *i.e.* a low purity kaolin. An essential part of this work was devoted to benchmarking the behaviour of mortars made with the new binder against that of conventional Portland cement mortars, to find similarities and differences between these two binder systems. This data should lay strong foundations towards the development of methodologies for the mix design of concrete made with low purity kaolin geopolymer binders, encouraging their popularisation and industrial acceptance. Such data can be of interest to the wider scientific community, designers and producers of concrete, as well as contractors, to better understand key mix proportion parameters affecting fundamental properties of geopolymer concrete formulated using a lithomarge based binder.

3 EXPERIMENTAL PROGRAMME

The research methodology is first outlined, followed by a short overview of the design of experiments technique (*i.e.* central composite design) which was adopted in the opening part of this work. Afterwards, the description of materials and mix proportions used is shown. Mortar mixing and sample preparation are then described, followed by the presentation of testing procedures.

3.1 Methodology

To satisfy the first objective, seven families of mortars, five GPMs and two PCMs, were tested. Their mix proportion parameters are reported in Table 1.

Table 1: Investigated mix proportion parameters and tested properties.

Mix family name	Mix proportion parameter			Properties tested
	w/s* or w/c** ratio [-]	Free water content [L/m^3]	Paste volume [L/m^3]	
GPM-0	Varied: 0.279–0.421*	Varied#	Varied: 439.5–510.4	Workability Setting time Compressive strength
GPM-1	Varied: 0.275–0.6*	Varied#	Kept constant at 500	Workability Compressive strength
GPM-2	Varied: 0.275–0.6*	Kept constant at 235	Varied#	Workability Compressive strength
GPM-3	Varied: 0.275–0.6*	Kept constant at 259	Varied#	Workability
GPM-4	Varied: 0.275–0.6*	Kept constant at 282	Varied#	Workability
PCM-1	Varied: 0.375–0.6**	Varied#	Kept constant at 500	Workability Compressive strength
PCM-2	Varied: 0.375–0.75**	Kept constant at 264	Varied#	Workability Compressive strength

– this mix parameter was varied to keep mix proportions yielding 1 m^3, but it was not a factor in the investigation.

Design of experiments (DoE) [25] approach was used to simultaneously investigate the influence of w/s ratio (factor A) and paste volume (factor B) on workability, setting times and compressive strengths of geopolymer mortars (GPMs) – mixes called GPM-0. The DoE approach has been chosen because it allows identification of the most influential factor(s) or factor interaction(s) affecting the investigated properties. Taking into account that the investigated properties were not expected to change linearly, the GPM-0 group of mortars was proportioned with a wide range of w/s ratios and paste volumes according to 2^2 full central composite design (CCD) plan, to obtain quadratic mathematical response models. A summary of the investigated levels of factors, in terms of actual and coded values (*i.e.* transformed actual values), is given in Table 2, while an overview of the CCD is presented in the subsequent section.

Table 2: Overview of investigated levels of experimental factors in actual and coded values for GPM-0 mortars.

Factor	**Level of factors in actual values**				
A: w/s ratio [-]	0.279	0.300	0.350	0.400	0.421
B: Paste volume [L/m^3]	439.6	450	475	500	510.4
Level of factors in coded values	-α	-1	0	+1	+α

In addition to the DoE work, workability and compressive strengths of GPMs were studied using a wider range of w/s ratios, *i.e.* from 0.275 to 0.6, either by keeping a constant paste volume or a free water content. For this range of w/s ratios, ten mortars were made with a constant paste volume of 500 L/m^3 (GPM-1) and another ten were made with a constant water content of 235 L/m^3 (GPM-2). To verify workability findings for GPM-2 mixes, two additional mortar families, *i.e.* GPM-3 and GPM-4, having a constant water content of 259 L/m^3 and 282 L/m^3, were investigated.

Behaviour of GPM-1 and GPM-2 mixes in fresh and hardened states was compared with that of two families of Portland cement-based mortars (PCMs): mixes proportioned with a constant paste volume of 500 L/m^3 (PCM-1) and with a constant water content of 264 L/m^3 (PCM-2). In the first case the w/c ratio was varied from 0.375 to 0.6 while in the second from 0.375 to 0.75. Significantly, from the preliminary tests it transpired that workable GPMs could be proportioned with lower water contents (resulting in relatively low w/s ratio) than the corresponding PCMs. In order to avoid mixes with a very low workability or dry mixes (slump of 0 mm), which would have to be rejected from the analysis of results as inconclusive, a minimum slump value of 5 mm was set. Therefore, after preliminary testing of both PCM and GPM mixes, the minimum w/c ratio for PCMs was intentionally set at 0.375 compared to a w/s ratio of 0.275 for GPMs. For the same reason, the free water content of PCM-2 proportioned with a constant water content was set at 264 L/m^3 compared to 235 L/m^3 for GPM-2. Water demands of the aluminosilicate precursor and Portland cement were also determined.

It is worth noting that for each family of mixes reported in Table 1, one of the mix proportion parameters was assigned with # symbol. These parameters had to be varied in order to keep the mortar mix proportions yielding 1 m^3. As such, they were not the subject of the investigation, but were reported in Table 1 for transparency.

To allow a like-for-like comparison, two GPM mixes and two PCM mixes were selected based on results obtained for all seven previously described families of mortars. The mortars had equivalent paste volumes (500 L/m^3) and characteristic compressive strengths to satisfy normal (37.5 MPa) and high strength (60 MPa) applications. They were tested for workability, setting time and compressive strength.

3.2 Central composite design (CCD)

DoE is a systematic and versatile tool for determining relationships among independent variables (factors) affecting a dependent variable (response) [25]. It allows for simultaneous investigation of a number of factors and for building of a mathematical model providing information on the effect of individual factors and factors' interactions on the studied response within previously defined boundaries of the experimental domain. Such statistically designed experiments based on factorial design are far more time- and labour-efficient than the "one-factor-at-a-time" approach.

The experimental plan was generated according to CCD, based on a two-level factorial design (2^k) to fit the second-order response surface model (RSM) to each studied property (Eq. 1) [25]. Because only two factors were investigated (k = 2), *i.e.* w/s ratio (factor A) and paste volume (factor B), a full CCD of 2^2 (2 factors each at 2 levels) was considered. The concept of CCD is presented below and is graphically depicted in Figure 1.

$$y = \beta_0 + \sum_{i=1}^{k} \beta_i x_i + \sum_{i=1}^{k} \beta_{ii} x_i^2 + \sum\sum_{i<j} \beta_{ij} x_i x_j + \in \qquad \textbf{Eq. 1}$$

where y is the response, β_0, β_i, β_{ii}, β_{ij} are regression coefficients, x_i, x_j are variables in coded values that represent levels of i-th and j-th factors (in given case they represent levels of factors A and B, respectively), $\sum_{i=1}^{k} \beta_i x_i$ is linear effect of i-th factor, $\sum_{i=1}^{k} \beta_{ii} x_i^2$ is quadratic effect of i-th factor, $\sum\sum_{i<j} \beta_{ij} x_i x_j$ is interaction effect of i-th and j-th factors, and $\in$ is a random error component representing the effects of uncontrolled variables in response y.

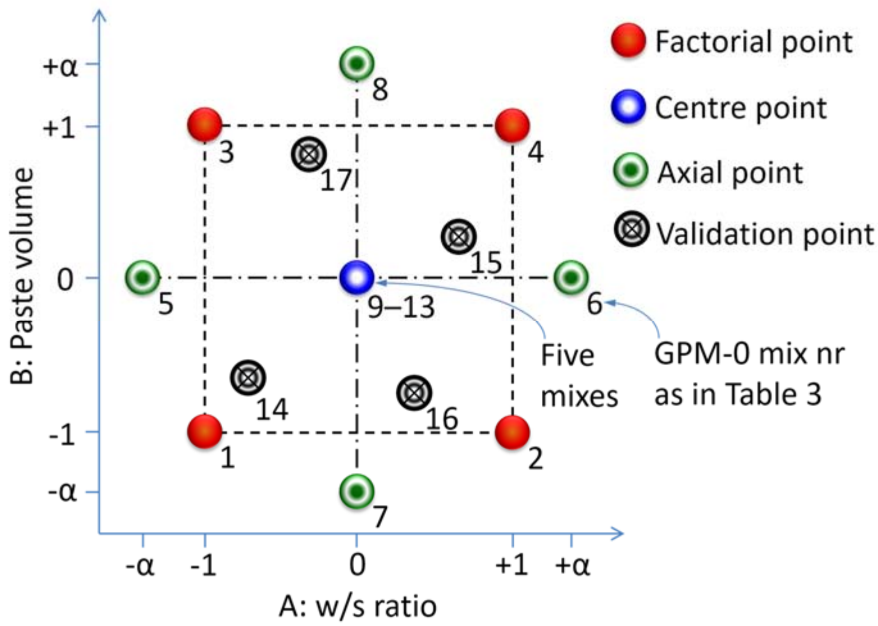

Figure 1: A graphical layout of the 2^2 CCD in coded values of factors for GPM-0 mixes.

The two-level factorial design with two factors (2^2) led to a total of four factorial runs (mixes 1 to 4 in Table 3). The low and the high levels of each factor were assigned coded values of *-1* and *+1* respectively. The centre point (mid-level) was assigned coded value of *0* for each factor (mixes 9 to 13 in Table 3). These five replicated mixes at the centre were used for evaluating the random error. The 2^2 factorial experimental design would result in a first-order (linear) model for the factors and their effects. In CCD, in order to obtain a second-order model (quadratic), additional experimental units are required. These are introduced by considering axial points, coded values of $\pm\alpha$, where $\alpha = (n_F)^{0.25}$ (n_F – a number of points used in the factorial portion of the design, in this case 4). Therefore, for each factor, two additional experimental units are considered (mixes 5 to 8 in Table 3), with their levels at $\pm\alpha$ from the centre point (in this case it was $\alpha = \pm 1.414$), and levels of all other factors fixed in the *0* level. This choice of the value of α ensured that the CCD was rotatable, *i.e.* the variance of predicted response is constant at all points that are the same distance from the centre point of the design [25].

Table 3 presents the low and high levels (coded *-1* and *+1*), the centre points (coded *0* for each factor), and the axial points (coded *-α* and *+α*) for each factor, resulting in a total of five levels for each factor. A model described by Eq. 1 may be used to represent the effects obtained for mixes 1 to 8. It is noteworthy that this equation contains a random error term ($\in$). As mentioned above, in order to estimate this error term five additional points were introduced, all replicating the centre point of all factors (mixes coded *0* for each factor – Table 3). Four randomly selected verification points (mixes 14 to 17 in Table 3) were used for checking the accuracy of developed models.

Table 3: Levels of experimental factors, given in actual and coded values, for GPM-0 mortars designed according to 2^2 CCD.

Type of points	GPM-0 mix nr	Actual values		Coded values	
		Factor A: w/s ratio [-]	Factor B: paste volume [L/m^3]	Factor A: w/s ratio [-]	Factor B: paste volume [-]
Factorial points	1	0.3	450	-1	-1
	2	0.4	450	1	-1
	3	0.3	500	-1	1
	4	0.4	500	1	1
Axial points	5	0.2793	475	-1.414	0
	6	0.4207	475	1.414	0
	7	0.35	439.6	0	-1.414
	8	0.35	510.4	0	1.414
Centre points	9	0.35	475	0	0
	10	0.35	475	0	0
	11	0.35	475	0	0
	12	0.35	475	0	0
	13	0.35	475	0	0
Validation points	14	0.3136	466.1	-0.728	-0.356
	15	0.3829	481.6	0.658	0.264
	16	0.3693	455.8	0.386	-0.768
	17	0.3341	495.4	-0.318	0.816

The levels of factors in Table 2 and Table 3 are shown in actual and coded values. Coding is a linear transformation of the original range of the dependent variable. It aids in the interpretation of the regression coefficients' fit to statistical model by introducing a relative size of a factor level. For a given factor, its level in coded value can be calculated as the difference between the level of factor in actual value and the value corresponding to the central point divided by half of the difference between the low and high levels of this factor. The equations for coding factors investigated in this work are shown in Eq. 2 and Eq. 3.

$$\text{w/s ratio in coded value} = \frac{\text{w/s ratio in actual value - 0.35}}{0.5 \cdot 0.1} \qquad \textbf{Eq. 2}$$

$$\text{Paste volume in coded value} = \frac{\text{paste volume in actual value - 475}}{0.5 \cdot 50} \qquad \textbf{Eq. 3}$$

3.3 Materials

The geopolymer binder used was a two component system produced by banah UK Ltd [26], *i.e.* an aluminosilicate precursor being the powder component and a chemical activator the liquid component. The aluminosilicate precursor was comprised of a calcined lithomarge and ground granulated blastfurnace slag (GGBS) at a fixed weight ratio of GGBS to calcined lithomarge of 0.142 [26]. The calcined lithomarge was manufactured by calcination of the altered basalt (lithomarge) at 750 °C in a rotary calciner and subsequent grinding in a ball mill [18-20]. The altered basalt was sourced from the IBF of the Antrim Lava Group (Northern Ireland). GGBS was produced by Civil & Marine Slag Cement Ltd. and conformed to BS EN 15167-1:2006 [27]. Portland cement CEM I 42.5N produced by Quinn Cement in Northern Ireland and conformed to the requirements of BS EN 197-1:2011 [28], was used. The chemical composition of the aluminosilicate precursor based on calcined lithomarge and Portland cement, determined using X-ray fluorescence spectrometry, are given in Table 4. X-ray powder diffraction patterns of the aluminosilicate precursor and Portland cement are given Figure 2. The main peaks in the XRD pattern of the aluminosilicate precursor are due to hematite, which is present as a result of calcination of goethite and magnetite in the original kaolinitic clay [18].

The Portland cement was found to be comprised of the following crystalline phases: alite, belite, aluminate, brownmillerite and gypsum. Particle size distributions (PSDs) of the aluminosilicate precursor and Portland cement are shown in Figure 3.

Table 4: Oxide composition and physical properties of the calcined lithomarge based aluminosilicate precursor and Portland cement.

Oxide composition [%]	Aluminosilicate precursor	Portland cement
SiO_2	32.04	20.21
Al_2O_3	24.99	4.79
Fe_2O_3	25.21	2.78
CaO	7.78	63.01
MgO	1.71	1.93
MnO	0.37	0.08
TiO_2	3.17	0.27
Na_2O	0.36	0.19
K_2O	0.15	0.59
SO_3	0.22	2.60
P_2O_5	0.14	0.12
LOI [%]	3.08	3.16
Specific gravity	2.89	3.13

An aqueous solution of potassium silicate with a water content of 41.2%, a SiO_2/K_2O molar ratio of 1.65 and specific gravity of 1.57, was used as a proprietary chemical activator for the lithomarge based precursor. Potable water from the mains supply (17 ±1 °C) was used as the mixing water.

Sand, rich in quartz and also containing albite, muscovite and clinochlore (as per XRD pattern shown in Figure 2), was sourced from Creagh's quarry (Creagh Concrete Products Ltd., Draperstown, Northern Ireland). The sand had oven-dry particle density of 2695 kg/m^3. Its water absorption at 1-h and 24-h was 0.92% and 1.1%, respectively. Both density and water absorption were determined according to BS 812-2:1995 [29]. The PSD of the sand was determined according to BS 812-103.1:1985 [30] and is shown in Figure 3.

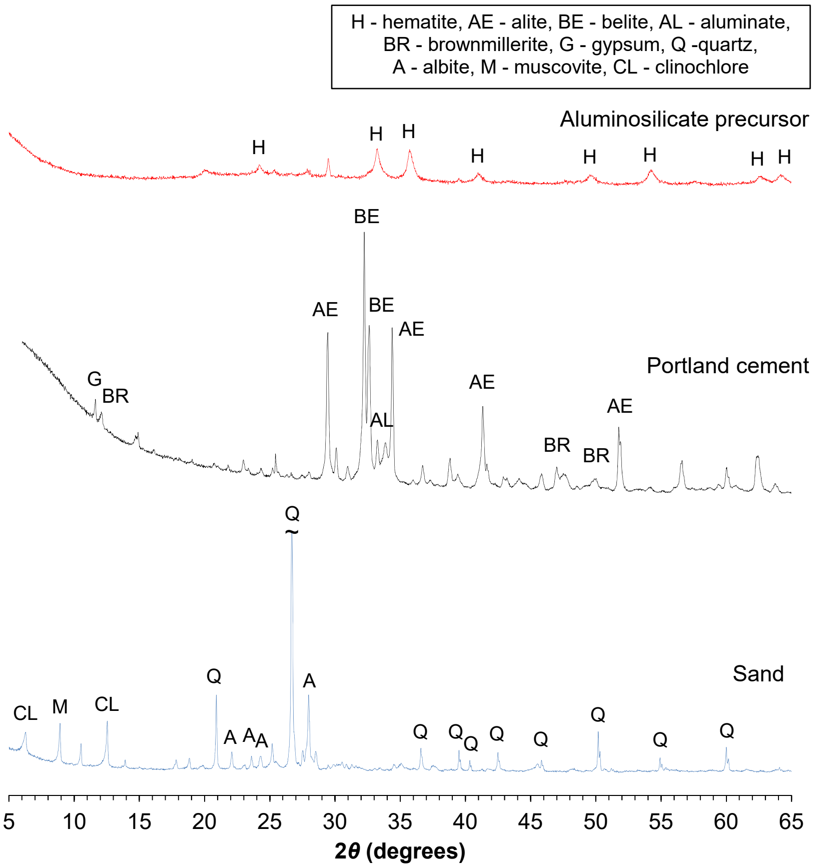

Figure 2: XRD patterns of the calcined lithomarge based aluminosilicate precursor, Portland cement and sand.

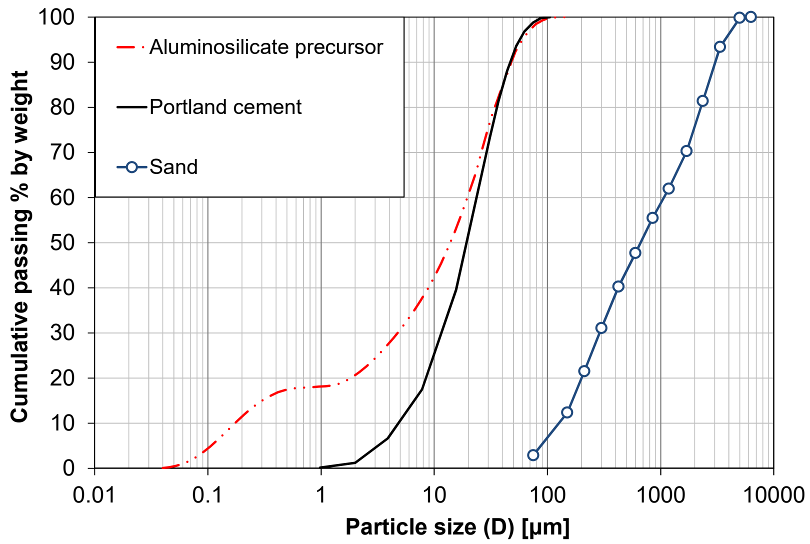

Figure 3: Particle size distribution of the calcined lithomarge based aluminosilicate precursor, Portland cement and sand.

3.4 Mortar proportions

The proportions of all GPM mixes are shown in Table 5 and those of PCM mixes in Table 6. Mix proportions of GPM-0 mixes are shown in the same order as in Table 3, while GPM-1, GPM-2, GPM-3, GPM-4, PCM-1 and PCM-2 mixes are organised with increasing w/s or w/c ratio. All GPMs had the same aluminosilicate precursor to chemical activator weight ratio of 1.41. All mortars were designed using the absolute volume method [31].

The paste volume was the sum of the volume of all materials in the mix with the exception of sand and 1-h absorption water. The w/s ratio for GPM was calculated according to Eq. 4, by dividing the total mass of free water in the paste portion of the mix by the total mass of solids in the paste. The w/c ratio for PCM was calculated using similar principle (Eq. 5).

$$w/s = \frac{m_{Fw}}{m_{s,paste}} = \frac{m_{Adw} - m_{Abw} + m_{w,act}}{m_{Prec} + m_{s,act}} \quad \textbf{Eq. 4}$$

$$w/c = \frac{m_{Fw}}{m_{PC}} = \frac{m_{Adw} - m_{Abw}}{m_{PC}} \quad \textbf{Eq. 5}$$

where m_{Fw} is the mass of free water, [kg], $m_{s,paste}$ is the total mass of solids in the paste, [kg], m_{Adw} is the total mass of added water during mortar mixing, [kg], m_{Abw} is the mass of water absorbed during aggregates pre-saturation, [kg], $m_{w,act}$ is the mass of water in the chemical activator, [kg], m_{Prec} is the mass of aluminosilicate precursor, [kg], $m_{s,act}$ is the mass of solids in the chemical activator (comprised mainly of alkali and silicate species), [kg], m_{PC} is the mass of Portland cement, [kg].

Table 5: Mix proportions of GPM-0, GPM-1, GPM-2, GPM-3, GPM-4 mixes.

Mix ID	w/s ratio	Paste volume [L/m³]	Material quantity per cubic metre [kg/m³]					
			Aluminosilicate precursor	Chemical activator	Sand	Absorption water	Total added water	Free water
GPM-0-1	0.300	450.0	483.8	343.2	1482.3	13.6	77.6	205.7
GPM-0-2	0.400	450.0	419.9	297.8	1482.3	13.6	128.6	238.0
GPM-0-3	0.300	500.0	537.6	381.3	1347.5	12.4	83.6	228.5
GPM-0-4	0.400	500.0	466.5	330.9	1347.5	12.4	140.2	264.4
GPM-0-5	0.279	475.0	527.6	374.2	1414.9	13.0	67.8	208.6
GPM-0-6	0.421	475.0	431.2	305.8	1414.9	13.0	143.5	257.2
GPM-0-7	0.350	439.6	439.2	311.5	1510.3	13.9	103.1	217.8
GPM-0-8	0.350	510.4	509.9	361.7	1319.5	12.1	115.8	252.9
GPM-0-9	0.350	475.0	474.6	336.6	1414.9	13.0	109.4	235.4
GPM-0-10	0.350	475.0	474.6	336.6	1414.9	13.0	109.4	235.4
GPM-0-11	0.350	475.0	474.6	336.6	1414.9	13.0	109.4	235.4
GPM-0-12	0.350	475.0	474.6	336.6	1414.9	13.0	109.4	235.4
GPM-0-13	0.350	475.0	474.6	336.6	1414.9	13.0	109.4	235.4
GPM-0-14	0.314	466.1	491.0	348.2	1438.9	13.2	87.9	218.2
GPM-0-15	0.383	481.6	459.7	326.1	1397.1	12.9	128.0	249.4
GPM-0-16	0.369	455.8	443.3	314.4	1466.6	13.5	115.9	232.0
GPM-0-17	0.334	495.4	506.3	359.1	1359.9	12.5	104.3	239.7
GPM-1-1	0.275	500	558.9	396.4	1347.5	12.4	66.9	217.8
GPM-1-2#	0.300	500	537.6	381.3	1347.5	12.4	83.8	228.5
GPM-1-3#	0.325	500	517.9	367.3	1347.5	12.4	99.6	238.5
GPM-1-4#	0.350	500	499.5	354.3	1347.5	12.4	114.2	247.7
GPM-1-5#	0.375	500	482.5	342.2	1347.5	12.4	127.8	256.4
GPM-1-6#	0.400	500	466.5	330.9	1347.5	12.4	140.5	264.4
GPM-1-7	0.450	500	437.6	310.4	1347.5	12.4	163.6	279.0
GPM-1-8	0.500	500	412.0	292.2	1347.5	12.4	183.9	291.9
GPM-1-9	0.550	500	389.3	276.1	1347.5	12.4	202.0	303.4
GPM-1-10	0.600	500	368.9	261.7	1347.5	12.4	218.3	313.7
GPM-2-1	0.275	540.3	603.9	428.3	1238.9	11.4	70.3	235.3
GPM-2-2	0.300	514.9	553.6	392.6	1307.3	12.0	85.6	235.3
GPM-2-3#	0.325	493.4	511.0	362.4	1365.3	12.6	98.6	235.3
GPM-2-4#	0.350	475.0	474.6	336.6	1414.9	13.0	109.7	235.3
GPM-2-5#	0.375	459.0	442.8	314.1	1458.0	13.4	119.3	235.3
GPM-2-6	0.400	445.0	415.2	294.5	1495.7	13.8	127.8	235.3
GPM-2-7	0.450	421.7	369.1	261.8	1558.5	14.3	141.8	235.3
GPM-2-8	0.500	403.1	332.2	236.6	1608.6	14.8	153.1	235.3
GPM-2-9	0.550	387.9	302.0	214.2	1649.6	15.2	162.3	235.3
GPM-2-10	0.600	375.1	276.7	196.3	1684.1	15.5	169.9	235.3
GPM-3-1*	0.275	594.1	664.1	471.0	1093.8	10.1	74.8	258.8
GPM-3-2*	0.325	542.6	561.9	398.6	1232.8	11.3	105.9	258.8
GPM-3-3*#	0.400	489.3	456.5	323.8	1376.2	12.7	138.1	258.8
GPM-3-4*	0.500	443.3	365.2	259.1	1500.5	13.8	165.9	258.8
GPM-3-5*	0.600	412.5	304.4	215.9	1583.3	14.6	184.4	258.8
GPM-4-1*	0.275	648.1	724.5	513.8	948.2	8.7	79.3	282.3
GPM-4-2*	0.325	591.9	613.1	434.8	1099.9	10.1	113.3	282.3
GPM-4-3*	0.400	533.9	498.1	353.3	1256.3	11.6	148.4	282.3
GPM-4-4*	0.500	483.5	398.4	282.6	1391.9	12.8	178.7	282.3
GPM-4-5*	0.600	450.0	332.1	235.5	1482.2	13.6	198.9	282.3

* – only workability was tested for these mixes, # – extra validation points for checking accuracy of models developed using CCD method.

Table 6: Mix proportions of PCM-1 and PCM-2 mixes.

Mix ID	w/c ratio	Paste volume [L/m³]	Material quantity per cubic metre [kg/m³]				
			Portland cement	Sand	Absorption water	Total added water	Free water
PCM-1-1	0.375	500.0	720.0	1347.5	12.4	282.4	270.0
PCM-1-2	0.400	500.0	694.9	1347.5	12.4	290.4	278.0
PCM-1-3	0.420	500.0	676.1	1347.5	12.4	296.4	284.0
PCM-1-4	0.450	500.0	649.8	1347.5	12.4	304.8	292.4
PCM-1-5	0.500	500.0	610.1	1347.5	12.4	317.5	305.1
PCM-1-6	0.550	500.0	575.1	1347.5	12.4	328.7	316.3
PCM-1-7	0.600	500.0	543.8	1347.5	12.4	338.7	326.3
PCM-2-1	0.375	489.1	704.3	1376.9	12.7	276.8	264.1
PCM-2-2	0.400	475.0	660.2	1414.9	13.0	277.1	264.1
PCM-2-3	0.450	451.6	586.9	1477.9	13.6	277.7	264.1
PCM-2-4	0.500	432.8	528.1	1528.6	14.1	278.2	264.1
PCM-2-5	0.550	417.5	480.2	1569.8	14.4	278.5	264.1
PCM-2-6	0.600	404.7	440.1	1604.3	14.8	278.9	264.1
PCM-2-7*	0.650	393.9	406.3	1633.4	15.0	279.1	264.1
PCM-2-8*	0.700	384.6	377.2	1658.5	15.3	279.4	264.1
PCM-2-9*	0.750	376.6	352.1	1680.0	15.5	279.6	264.1

* – only workability was tested for these mixes.

3.5 Mix preparation

All constituent materials, except mixing water (17 ±1 °C), were stored in dry locations at room temperature (20 ±2 °C) prior to batching to ensure that no other parameters influenced the results. Sand was oven-dried (105 ±5 °C) for over 48 hours until a constant mass was reached, subsequently cooled and stored in sealed plastic bags until mixing. All mixes were batched following exactly their pre-determined mix proportions, *i.e.* no additional water (other than what is given in the mix design) was added during mixing. Mixes listed in Table 5 and Table 6 were prepared in a randomised order to minimise the experimental error.

All mortar mixes were prepared in a 10 L capacity planar-action high-shear mixer in batches of 3.7 L. The mixing procedure consisted of the following steps:

- **Step 1** − Pre-saturation of sand started 15 minutes before the actual mortar mixing (Step 2). The dry portion of sand was placed in the mixer's pan with ½ of the total added water (free + absorption water) and mixed for approximately 1 minute.

- **Step 2** − The dry portion of binding material, *i.e.* aluminosilicate precursor or Portland cement, was introduced into the mixing bowl followed by 1 minute of mixing.
- **Step 3** – Addition of the remaining water (free + pre-saturation water) and, in the case of GPMs, addition of the chemical activator followed by 2 minutes of mixing at a low speed. The beginning of this step is referred to as time zero.
- **Step 4** – Stopping of the mixer for 1 minute to crush any lumps of remaining solids.
- **Step 5** – Mixing for 2 minutes at a high speed.
- **Step 6** – Mixing for 1 minute at a low speed.

3.6 Sample casting, demoulding and conditioning

All mortar specimens were cast in two layers. Each layer was compacted on a vibrating table. After casting, the moulds with samples were wrapped with cling film to prevent water evaporation and placed in the conditioning room (RH >95% and 20 ±1 °C). Samples were demoulded at 24 ±0.5 hours, counting from time zero, and placed in plastic boxes on 15 mm height spacers. Boxes were filled with water to the height of 5 mm, then covered with tightly fitting lids and stored in the conditioning room (20 ±1 °C). This procedure allowed the conditioning of the samples at RH of >95%, prevented unintentional carbonation of the samples and leaching of alkalis.

3.7 Test techniques

Workability – the slump test and the flow table test commenced immediately after the end of mixing (approximately 7 min after time zero). A metal cone-shaped mould described in BS 6463-103:1999 [32] (90 mm in height, wider bottom end with 66 mm internal diameter and narrower top end with 38 mm internal diameter), was placed in the centre of a flow table disk.

The mould was filled with mortar in three layers. Each layer was compacted by 10 short strokes of a metal bar (10 mm in diameter). Then the conical mould was gently lifted (approximately 30 s after the finishing of mortar placing), and the slump of the mortar was measured (following the same procedure as for the concrete slump test [33]) and reported in mm. Immediately after the slump measurement, the mortar sample was subjected to 15 table jolts. The mortar spread was measured in two perpendicular directions and the average was reported as the mortar flow in mm. The above test procedure was very similar to that used for the determination of consistence of mortar mixes (*i.e.* mortar flow using a flow table), described in BS EN 13395-1:2002 [34]. The two dissimilarities were: (i) a conical mould with different dimensions (as reported above) was used in present study, which allowed for measurement slump of fresh mortar sample, and (ii) the jolting of the sample was not applied immediately after the cone-shape mould was lifted, but it started after the slump reading was taken (*i.e.* it was delayed by approximately 30 s).

Water demand – the water demand of the aluminosilicate precursor and Portland cement was determined by testing slurries/pastes with varying water-to-powder (w/p) ratio or w/c ratio, similar to the method described in [**Error! Reference source not found.**]. The conical mould, used for testing workability of mortars (see previous paragraph), was placed in the middle of a Plexiglas table (400 mm in diameter). Slurry was placed (poured) in the mould. Then the conical mould was gently lifted (approximately 10 s after completing the slurry/paste placement). Once the flow stopped, the slurry/paste spread was measured in two perpendicular directions and the average was reported as the flow in mm. Average spread results (y-axis) were plotted against the w/c ratios and w/p ratios (x-axis). The minimum w/p or w/c ratio required to initiate the flow (indicating the water demand of the aluminosilicate precursor or Portland cement, respectively) was determined as the intersection of a line fitted to the experimental data with a horizontal line corresponding to the internal diameter of the wider (bottom) end of the conical mould (66 mm in diameter).

Setting time – initial and final setting times of mortars were determined by the penetration resistance method described in ASTM C403 [36]. Samples for setting time were cast and compacted in the same way as the cubes for compressive strength determination. Samples were left in the conditioning room at 20 ±1 °C and between testing were covered to prevent water evaporation. At least eight penetrations were performed on the sample using a range of standarised needles (with surface area of 651, 326, 160, 65, 32 and 16 mm^2) to obtain a resistance of the mortar to penetration. In order to obtain the minimum required number of penetration values, the intervals between subsequent penetrations were adjusted as necessary, which depended upon the rate of setting. The bearing surface of the needle was brought into contact with the sample surface. Then, within 10 ±2 s, a uniform vertical force was applied on the penetrometer to drive the needle into the sample to a depth of 25 ±2 mm. The force required to penetrate the sample and the elapsed time after time zero were recorded. The recorded force was divided by the surface area of the testing needle to obtain the penetration resistance [MPa] of the mortar at given time. Penetration resistance results were plotted against elapsed time. For each mix, the times of initial and final setting (counting from time zero) were determined as the times when the penetration resistance equalled 3.5 and 27.6 MPa, respectively. Setting time results are reported in minutes, as the elapsed time after time zero.

Compressive strength – the compressive strength of mortar specimens at a given age were determined by crushing three 50×50×50 mm cubes each time using a similar procedure to that given in BS EN 12390-3:2009 [37] (to reflect sample size, a proportionally lower loading rate of 50 kN/min was used). The applied load [kN] was divided by the test sample surface area

[mm^2] to calculate the compressive strength [MPa]. An average of the three measurements was reported.

4 RESULTS AND DISCUSSION

The development of statistical models for workability, setting times and strengths of GPM mixes proportioned using CCD methodology (GPM-0) will be outlined first followed by the evaluation of to the repeatability and accuracy of the developed models. Models developed for GPM-0 mixes will then be discussed, followed by the presentation and discussion of results obtained for GPM and PCM mixes formulated with either constant paste volume (GPM-1 and PCM-1) or constant water content (GPM-2, GPM-3, GPM-4 and PCM-2). Finally, a direct comparison of workability, setting times and compressive strengths of selected GPM and PCM mixes, having the same paste volume and strength grade, will be presented.

4.1 Response surface models development and validation

Response surface models (RSMs), *i.e.* statistical models, were developed by multi-regression analyses, based on results presented in Table 7, using a statistical software package Design Expert [38]. Analysis of variance (ANOVA) was carried out to test the significance of regression models and their regression coefficients. *F*-test and *t*-test were performed to identify the nonsignificant (NS) variables, which were subsequently eliminated from derived models (step-by-step process with the most nonsignificant effects first). Probability values below 0.05 were considered as significant evidence that the factor's effects or the effect of factors' interactions have a highly significant influence on the modelled response, while values above 0.10 suggest no significant effect. All these statistical tools rely on the assumption that data is normally distributed. Therefore, before undertaking ANOVA, responses were checked for normality using the Shapiro-Wilk test [39]. For results that were not normally distributed, the

Cox-Box method [40] was used to identify an appropriate power-based transformation, which was then applied to the data.

Table 7: Results for GPM-0 mixes.

Mix ID	w/s ratio	Paste volume [L/m^3]	Slump [mm]	Flow [mm]	Setting time [min]		Compressive strength [MPa]		
					Initial	Final	1-day	7-day	28-day
GPM-0-1	0.300	450.0	15	110.0	69	89	36.1	65.3	70.5
GPM-0-2	0.400	450.0	67	189.5	117	145	19.6	41.2	49.6
GPM-0-3	0.300	500.0	55	139.0	72	85	37.1	60.2	69.2
GPM-0-4	0.400	500.0	78	211.5	90	112	20.7	42.8	49.7
GPM-0-5	0.279	475.0	6	95.5	46	59	40.7	60.1	68.4
GPM-0-6	0.421	475.0	78	206.0	100	123	17.3	35.2	41.9
GPM-0-7	0.350	439.6	38	137.0	75	91	24.8	53.3	59.4
GPM-0-8	0.350	510.4	73	181.5	92	112	26.8	52.7	53.3
GPM-0-9	0.350	475.0	69	173.5	89	115	25.4	51.9	55.6
GPM-0-10	0.350	475.0	69	166.0	87	104	26.9	53.0	52.4
GPM-0-11	0.350	475.0	64	161.0	83	104	26.9	48.7	60.6
GPM-0-12	0.350	475.0	67	175.5	80	102	29.2	53.3	56.0
GPM-0-13	0.350	475.0	68	172.0	91	116	29.9	51.5	61.8
GPM-0-14	0.3136	466.1	57	141.5	74	92	33.9	67.0	71.9
GPM-0-15	0.3829	481.6	76	201.0	83	107	21.7	48.2	53.6
GPM-0-16	0.3693	455.8	70	181.0	83	107	24.3	47.6	56.2
GPM-0-17	0.3341	495.4	72	192.0	72	90	30.7	58.9	67.2

Derived RSMs for each measured response are given by Eq. 6–12 (where, x_A and x_B represent levels of coded values of factors A and B, respectively). Applied transformation, correlation coefficients, parameter estimates, and probability values (*P* value) of the RSMs are shown in Table 8. Models are valid only within the main investigated experimental domain, *i.e.* in the range between -1 and +1 of coded values of each factor. Most of the models had high correlation coefficients (R^2 >0.85), thus indicating a good correlation between predicted values (calculated with developed RSMs) and experimental results.

$$(\text{Slump})^{1.5} = 553.5 + 215.6 \cdot x_A + 130.1 \cdot x_B - 52.3 \cdot x_A \cdot x_B - 92.0 \cdot x_A^2 - 53.4 \cdot x_B^2 \quad \textbf{Eq. 6}$$

$$\text{Flow} = 167.3 + 38.5 \cdot x_A + 14.2 \cdot x_B - 7.1 \cdot x_A^2 \quad \textbf{Eq. 7}$$

$$\text{Initial setting time} = 84.0 + 17.7 \cdot x_A \quad \textbf{Eq. 8}$$

$$\text{Final setting time} = 104.3 + 22.0 \cdot x_A \quad \textbf{Eq. 9}$$

$$\text{Ln(1-day compressive strength)} = 3.296 - 0.300 \cdot x_A \quad \textbf{Eq. 10}$$

$$\text{Ln(7-day compressive strength)} = 3.960 - 0.195 \cdot x_A - 0.051 \cdot x_A^2 \quad \textbf{Eq. 11}$$

$$\text{28-day compressive strength} = 57.6 - 9.7 \cdot x_A \quad \textbf{Eq. 12}$$

Table 8: Parameter estimates of derived models for mixes GPM-0.

Property	**Slump**		**Flow**		**Initial setting time**		**Final setting time**		**1-day compressive strength**		**7-day compressive strength**		**28-day compressive strength**	
Transformation	$(\text{Slump})^{1.5}$		None		None		None		Ln(1-day f_c)		Ln(7-day f_c)		None	
R^2	0.98		0.97		0.74		0.72		0.96		0.95		0.87	
Effect	Estimated coefficient	*P value*	Estimated coefficient	*P value*	Estimated coefficient	*P value*	Estimated coefficient	*P value*	Estimated coefficient	*P value*	Estimated coefficient	*P value*	Estimated coefficient	*P value*
Intercept (β_0)	553.5	-	167.3	-	84.0	-	104.3	-	3.296	-	3.960	-	57.6	-
Main effect of factor A (β_A)	215.6	*< 0.0001*	38.5	*< 0.0001*	17.7	*0.0002*	22.0	*0.0002*	-0.300	*< 0.0001*	-0.195	*< 0.0001*	-9.7	*< 0.0001*
Main effect of factor B (β_B)	130.1	*< 0.0001*	14.2	*< 0.0001*	NS	*NS*	NS	*NS*	NS	*NS*	NS	*NS*	NS	*NS*
Interaction A×B (β_{AB})	-52.3	*0.0260*	NS	*NS*	NS	*NS*	NS	*NS*	NS	*NS*	NS	*NS*	NS	*NS*
Quadratic effect of factor A (β_{AA})	-92.0	*0.0003*	-7.1	*0.0154*	NS	*NS*	NS	*NS*	NS	*NS*	-0.051	*0.0065*	NS	*NS*
Quadratic effect of factor B (β_{BB})	-53.4	*0.0068*	NS	*NS*	NS	*NS*	NS	*NS*	NS	*NS*	NS	*NS*	NS	*NS*

NS – nonsignificant effect.

In order to quantify the repeatability of data, results obtained for the five centre points were statistically analysed. Table 9 reports the mean value, $\bar{x}$, the sample standard deviation, s_d, the coefficient of variation (COV), the estimated error with 95% confidence limit, $E_{E95\%}$, and the relative error, E_R. For all responses COV was below 10%, indicating good repeatability.

Table 9: Repeatability of test results for the five centre points of GPM-0 mixes.

Statistical parameters (see description below)	Slump [mm]	Flow [mm]	Setting time [min]		Compressive strength [MPa]		
			Initial	Final	1-day	7-day	28-day
$\bar{x} = \frac{\sum_{i=1}^{n} x_i}{n}$, [*]	67.4	169.6	86.1	108.1	27.6	51.7	57.3
$s_d = \sqrt{\frac{\sum_{i=1}^{n}(x_i - \bar{x})^2}{n-1}}$, [*]	2.1	6.0	4.5	6.7	1.8	1.8	3.9
$COV = 100\% \cdot \frac{s_d}{\bar{x}}$, [%]	3.1	3.5	5.3	6.2	6.7	3.5	6.8
$E_{E95\%} = \frac{t_{\alpha/2,v-1} \cdot s_d}{\sqrt{n}}$, [*]	2.6	7.4	5.6	8.3	2.3	2.3	4.8
$E_R = 100\% \frac{E_{E95\%}}{\bar{x}}$, [%]	3.8	4.4	6.5	7.7	8.3	4.4	8.4

Where $\bar{x}$ is the arithmetic mean value of five centre observations $x_9, x_{10}, \ldots x_{13}$, n is the size of the sample (n = 5), s_d is the sample standard deviation, $E_{E95\%}$ is the estimated error with 95% confidence limit, $t_{\alpha/2,v-1}$ is the percentage point of the t distribution, α is the confidence level ($\alpha = 0.05$), v are the degrees of freedom ($v = 5$), E_R is the relative error.

* – value in given unit.

Accuracy of developed models was checked by comparing predicted-to-measured values obtained with four randomly selected verification mortar mixes (GPM-0-14 – GPM-0-17). In addition, nine mixes (five from GPM-1 family: GPM-1-2 – GPM-1-6, three from GPM-2 family, GPM-2-3 – GPM-2-5, and one mix from GPM-3 family: GPM-3-3) made with w/s ratios and paste volumes which fitted the main experimental domain of the CCD plan were used as extra validation points. The predicted-to-measured values for five centre points, four validation points and nine extra validation points are shown in Figure 4. All figures show the identity line (1:1 line for predicted values) and the estimated error at a 95% confidence limits calculated for the five centre points (using values given in Table 9). It was assumed that the error was random and normally distributed, so the residual terms representing the difference between the predicted and actual values should exhibit similar properties [25]. Data points below the identity line indicate that the derived statistical model overestimates the measured values, while those above the line indicate an underestimation of the measured values. The average ratios between predicted and measured value, calculated for four validation points, for slump, flow, initial setting time, final setting time, 1-day strength, 7-day strength and 28-day strength were 0.90, 0.92, 1.07, 1.05, 0.99, 0.94 and 0.93, respectively. The average ratios calculated for all thirteen validation points for slump and flow, and twelve validation points for 1-, 7- and 28-day strengths, were 0.97, 0.95, 0.89, 0.97, and 1.01, respectively. Both sets of ratios indicate good accuracy of the derived statistical models.

It is important to emphasise that the developed RSM models are valid for a given set of materials. Substantial changes in the materials used (*e.g.* discrepancies in chemical composition and/or physical properties) will require validation of these models. Preliminary validation can be performed by examining the accuracy of the proposed models, *i.e.* comparing the difference between predicted values (obtained using the developed models) and the measured values obtained for the validated variable, *e.g.* new source of lithomarge.

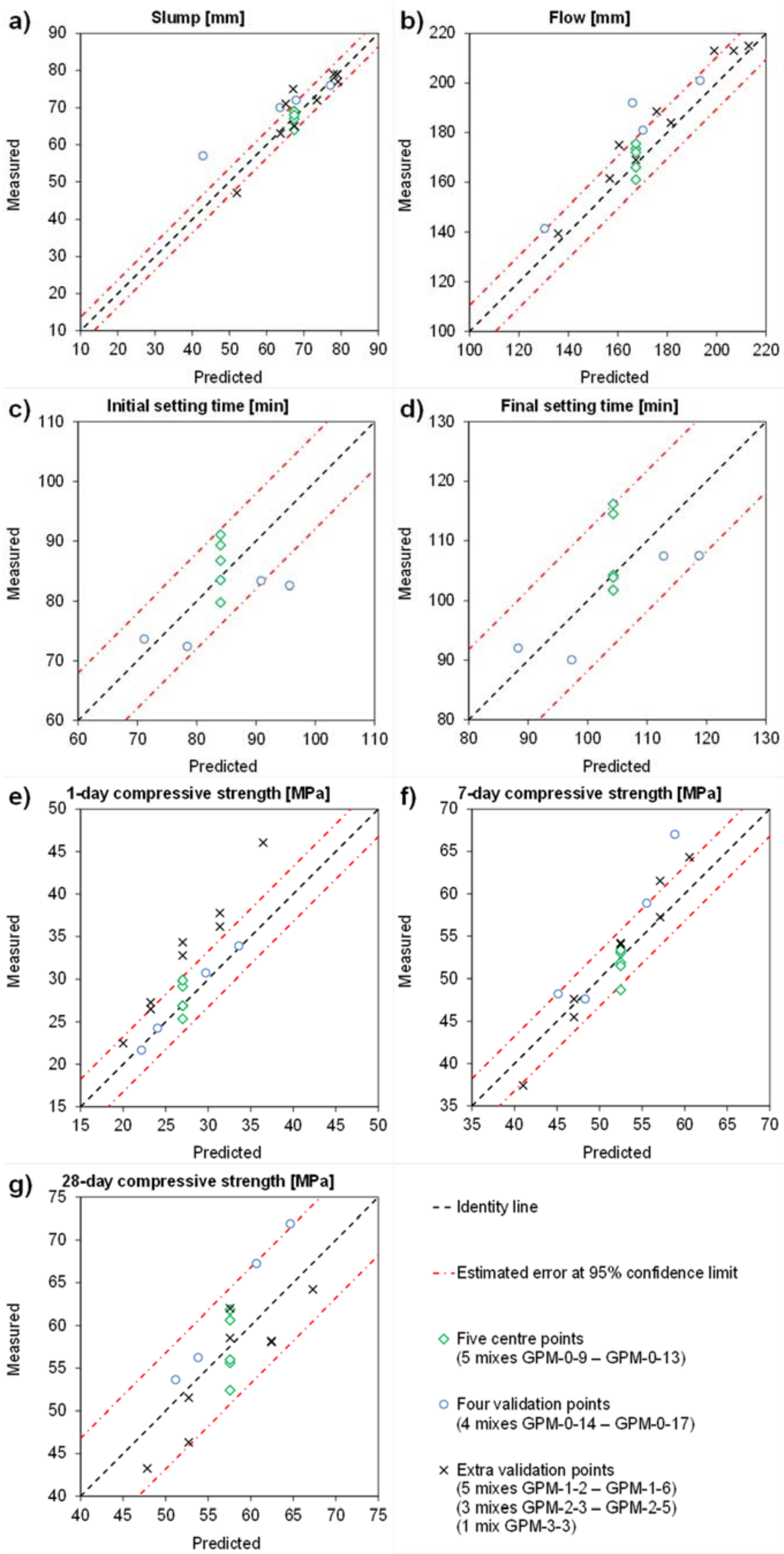

Figure 4: Predicted *vs.* measured values of investigated properties of GPM-0 mixes.

4.2 Influence of mix proportion parameters on the behaviour of geopolymer and Portland cement mortars.

4.2.1 Workability

Information on the workability of GPM-0 mixes, designed according to CCD methodology, can be gained from the developed RSMs given by Eq. 6 and Eq. 7. Contour plots of the slump and flow models, in the coordinates of the two investigated factors, *viz.* w/s ratio and paste volume, are shown in Figure 5a and Figure 5b, respectively. RSMs indicate that workability depended on both w/s ratio and paste volume. As expected, an increase in either of these factors caused an increase in slump and flow values. When the main effects of both factors are concerned, an increase in w/s ratio had *ca.* 1.7 times and 2.7 times higher impact on the value of slump and flow, respectively, than an increase in the paste volume. Higher order effects (*i.e.* β_{AB}, β_{AA} and β_{BB} – see Table 8, Eq. 6 and Eq. 7), if significant, caused a decrease in the slump and flow of GPM-0 mixes.

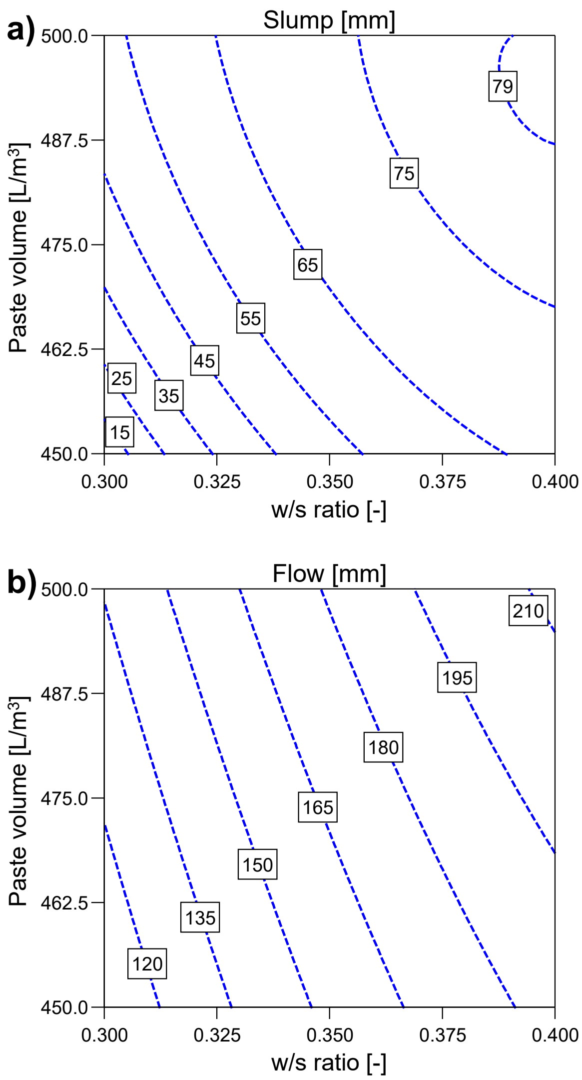

Figure 5: Contour plots developed for a) slump and b) flow of GPM-0 mixes.

The slump and flow results of all five families of geopolymer mortars (GPM-0, GPM-1, GPM-2, GPM-3 and GPM-4) and two of the cement-based mortars (PCM-1 and PCM-2) are shown in Figure 6 and Figure 7, respectively.

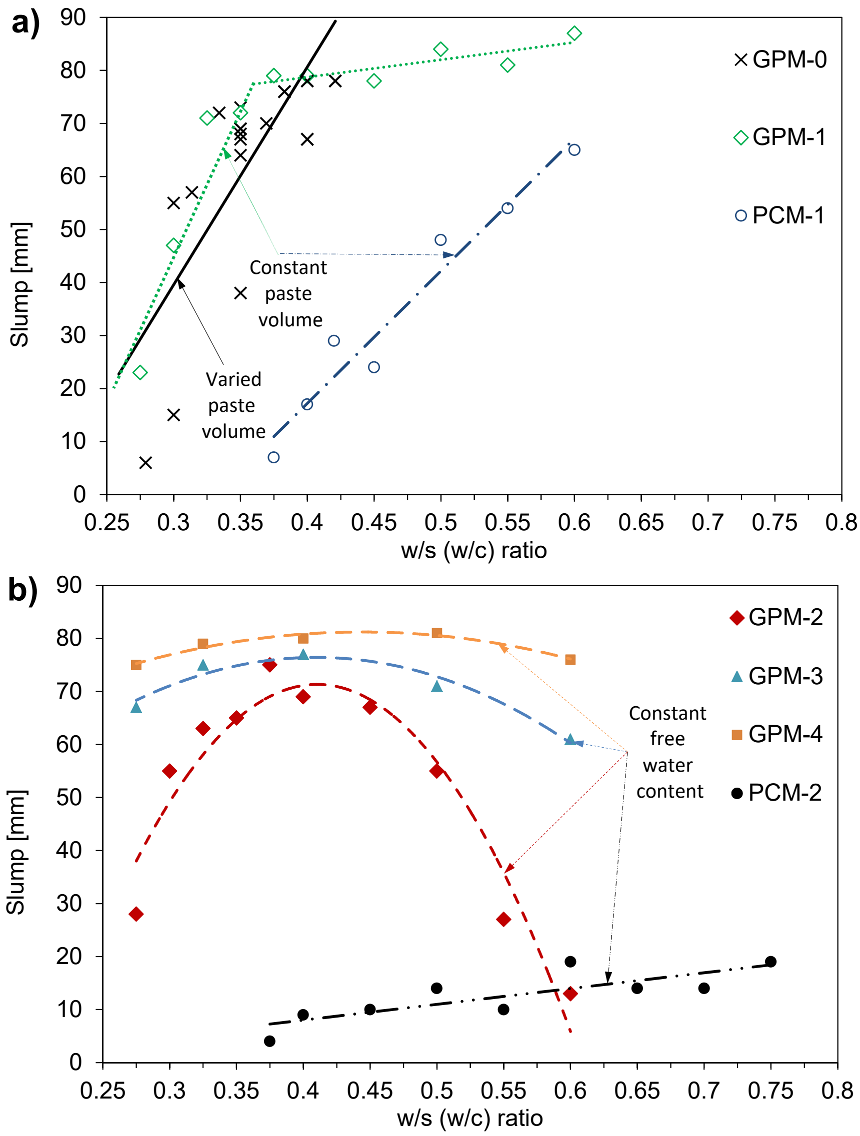

Figure 6: Influence of w/s ratio and w/c ratio on the slump of GPM and PCM mixes respectively, made with a) a constant and varied paste volume, and b) a constant free water content.

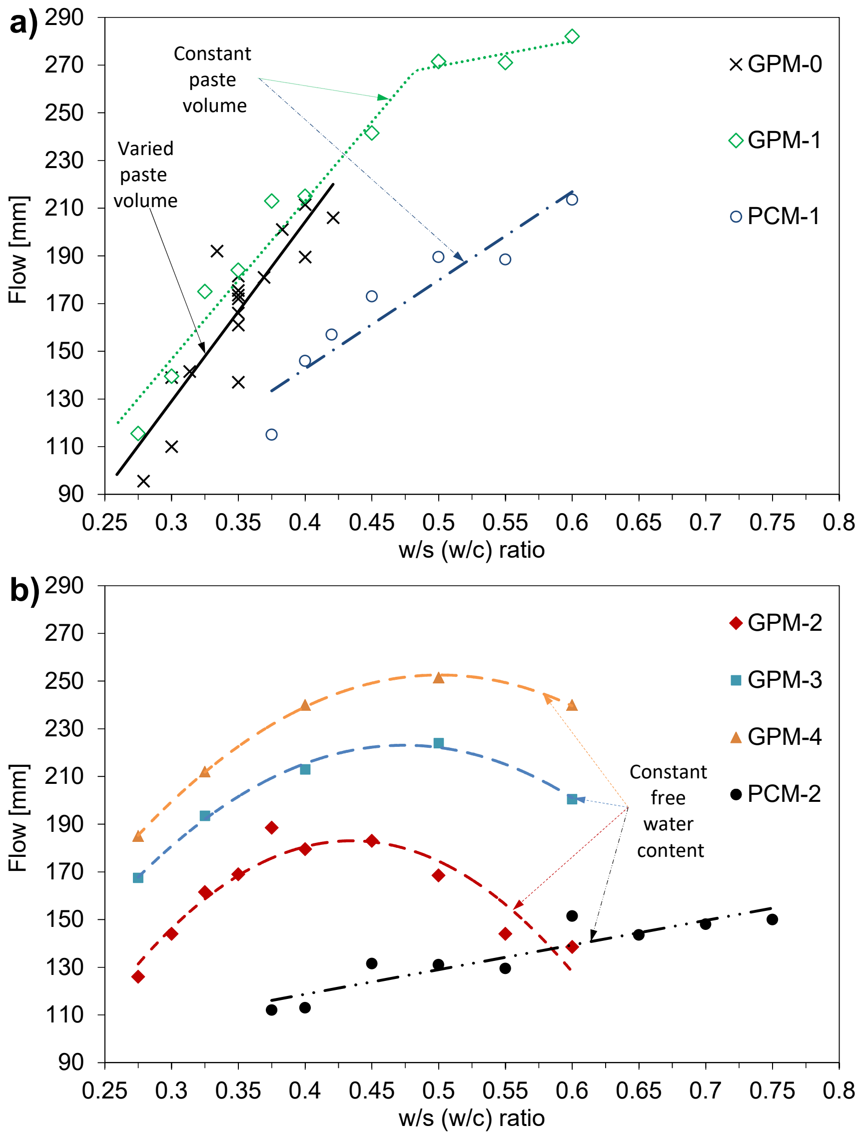

Figure 7: Influence of w/s ratio and w/c ratio on the flow of GPM and PCM mixes respectively, made with a) a constant and varied paste volume, and b) a constant free water content.

As expected, an increase in the w/c ratio for PCM-1 mixes, *i.e.* mortars made with constant paste volume of 500 L/m^3, resulted in a large increase in slump (Figure 6a) and flow (Figure 7a) values. Since the paste volume was fixed, an increase in the w/c ratio resulted in the increase in the free water content of these mortars (Table 6) and a simultaneous decrease in the content of cement causing coarsening of the overall PSD of the mixes (Figure 8c). In the case of the PCM-2 mortars, proportioned with a constant water content of 264 L/m^3, an increase in the w/c ratio resulted in a slight increase in slump (Figure 6b) and flow (Figure 7b) values. As shown in Table 6, for PCM-2 mixes an increase in the w/c ratio resulted in a decrease of the cement content and simultaneous increase in the sand content. For that reason, with an increase in w/c ratio, the surface area of solids (cement and sand) to be lubricated with water was reduced (see coarsening of the overall PSD of the mixes in Figure 8d), hence the mortar showed a slight improvement in workability. Both trends were as expected, and in good agreement with the literature [24], [41], [42].

For GPM-1 mixes, proportioned with a constant paste volume of 500 L/m^3, an increase in w/s ratio up to a value of *ca.* 0.375 resulted in a sharp increase in slump (Figure 6a). Further increases in w/s ratio resulted in minor changes in slump (for w/s ratios between 0.375 and 0.6 the slump varied in the range of 78–87 mm). Results obtained for flow of GPM-1 mixes show similar trend to that of slump, however, the transition between sharp increase in flow and plateau appears to be around w/s ratio of 0.5 (Figure 7a). The plateaus observed for the slump and flow results indicate that the upper range limits of these tests were approached. Nevertheless, the explanation given in previous paragraph for trends observed for PCM-1 mixes is also valid for the increase in both slump and flow values of GPM-1 mixes. Specifically, for GPM-1 mixes an increase in the w/s ratio led to an increase in free water content and a decrease in binder content (expressed as $m_{s,paste}$ in Eq. 4), causing the overall PSD of the mixes to coarsen (see Table 5 for mix proportions and Figure 8a for the overall PSDs of GPM-1 mixes).

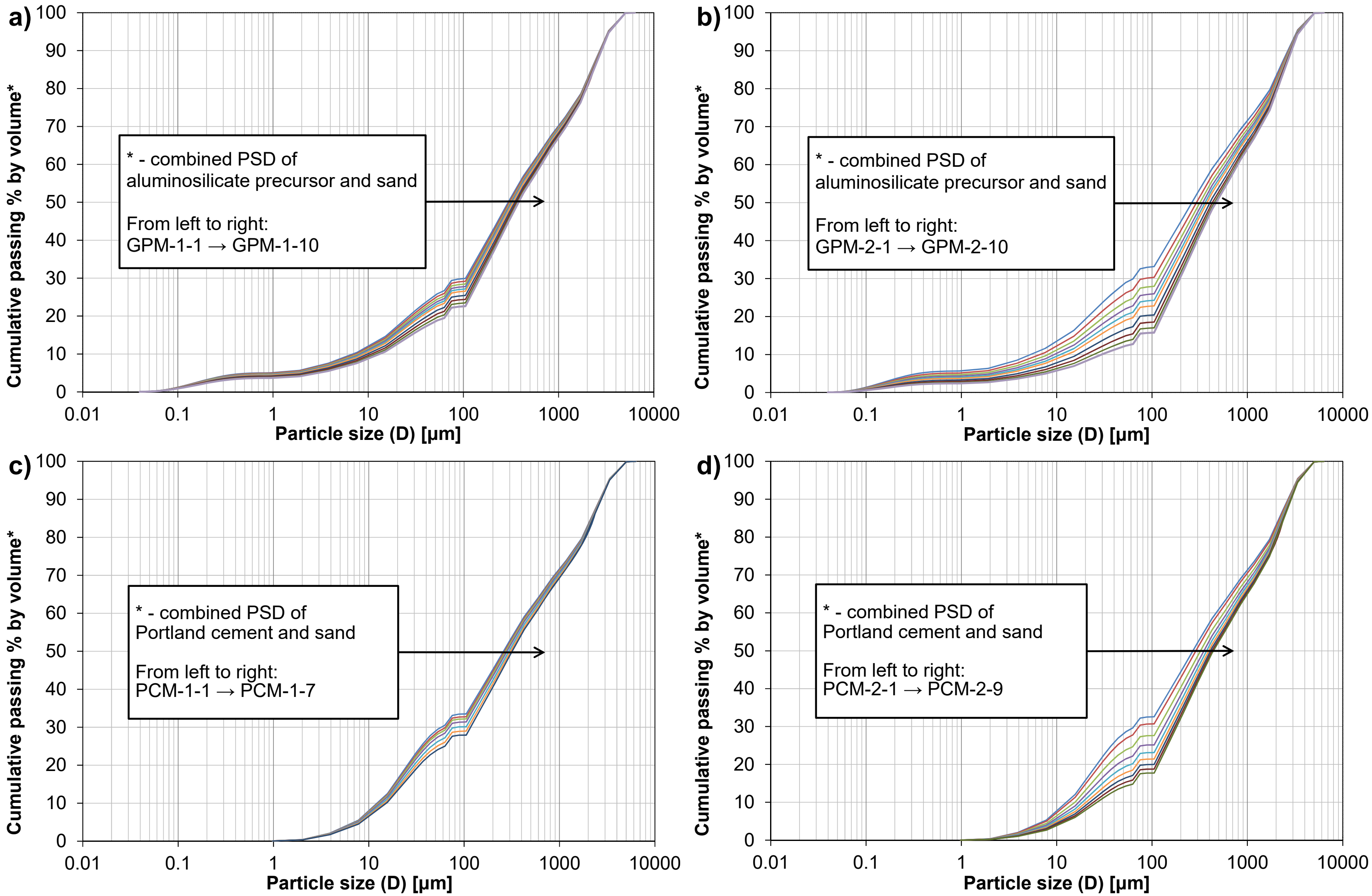

Figure 8: Overall particle size distributions of a) GPM-1 mixes, b) GPM-2 mixes, c) PCM-1 mixes and d) PCM-2 mixes.

In the case of GPM-2 mixes, made with a constant free water content, the slump and flow initially increased with an increase in the w/s ratio, reaching a maximum value at a w/s ratio of *ca.* 0.4–0.45 (see Figure 6b and Figure 7b, respectively). Further increases in the w/s ratio led to a decrease in the value of both properties. These trends were most likely the result of:

- The quantity of paste available for lubrication of sand.
- The content of free water available for the geopolymerisation process.

Where the first cause is concerned, a general concept of filling the space between aggregate particles with paste is applicable [43]. As shown in Table 5, as a result of the constant water content of GPM-2 mixes, an increase in w/s ratio resulted in a decrease in paste volume from approximately 540 to 375 L/m^3 (*i.e.* a decrease in aluminosilicate precursor content and simultaneous increase in sand content caused coarsening of the overall PSD of the mixes – see Figure 8b). Therefore, with the increase in the w/s ratio there was gradual increase in volume of sand, hence an increase in surface area of sand to be lubricated with paste. Using the void content measurement method described in BS 812-2:1995 [29], it was found that for the sand used, the voids in a loose oven-dried state equated to *ca*. 38% (380 L/m^3). GPM-2 mixes with w/s ratios of 0.5, 0.55 and 0.6 had a paste volume of 403, 388 and 375 L/m^3, which is relatively close to what would be required to fill the voids between sand particles in the loose oven-dried state. Portland cement based-mixes (PCM-2) proportioned with w/c ratio of 0.6–0.75 had a comparable paste volume (in the range of 405–377 L/m^3) to the three GPM-2 mixes, but this relatively low paste volume did not translate to any negative influence on slump (Figure 6b) or flow (Figure 7b). It is also important to note that workability trends similar to that observed for the GPM-2 mixes were also seen for GPM-3 and GPM-4 families of mixes (Figure 6b and Figure 7b). As for GPM-2 mixes, these two families of GPMs were tested in order to evaluate the effect of w/s ratio on workability at a constant free water content, but they were proportioned with reduced sand contents. GPM-3 and GPM-4 families of mixes were made with the same w/s ratio range as GPM-2 mixes (0.275 and 0.6), but the free water contents were intentionally set at higher dosages (fixed at 259 and 282 L/m^3, respectively). Obviously, the increase in free water contents led to lowered sand contents, and in turn resulted in higher paste volumes for GPM-3 and GPM-4 than those calculated for GPM-2 mixes (see Table 5). As a consequence, GPM-3 and GPM-4 mixes showed higher workability values than their GPM-2 counterparts. Based on the above evidence, the trends observed for GPM-2, GPM-3 and GPM-4 cannot be solely explained with the concept of filling the space between the aggregate particles with paste.

The second proposed cause can be explained using the conceptual geopolymerisation process proposed by Duxon *el al.* [44] and the work of Zuhua *et al*. [45]. During the addition of activator to the powder portion of the binder, silicates present in the activator, as well as alumina and silica from the powder portion of the binder (rapidly dissolved due to the high pH of the activator), form a supersaturated aqueous mixture of silicate, aluminate and aluminosilicate species. In the first phase of geopolymerisation, a part of the added free water is used to facilitate the dissolution and hydrolysis process of these aluminosilicate compounds [45]. In the second phase, hydrolysis and polycondensation of different aluminate- and silicate-hydroxyl species in the supersaturated aqueous mixture leads to the formation of a gel (*i.e.* setting and microstructure formation), and water consumed during dissolution is released [44, 45]. These two phases can co-exist [45]. In this work, the slump and flow were measured between 7th and 10th minute after time zero, hence are mostly concerned with the first stage of the geopolymerisation process (dissolution and hydrolysis). Therefore, it was assumed that water release due to polycondensation had not yet taken place at the time of the workability measurement.

Zuhua et al. [45] postulated that both water content and alkali concentration (alkalinity) in the activator play an important role during the polymerisation process (geopolymer mixes composed of calcined kaolin and sodium-based activator $Na_2O \cdot 1.2SiO_2$ of 35 wt.% were tested). Specifically, when alkalinity is high, the high water content increases the initial reaction rate (associated with water consumption for dissolution and hydrolysis of aluminosilicates). When studying metakaolin systems with different water contents, Yao *et al*. [46] observed that excess content of water diluted the activator (lowered concentration of OH^-), hindering the ability of the activator to dissolve the precursor. Further evidence was provided by Rahier *et al.* [47], confirming that at low and high water contents the geopolymer reaction rate was decreased, with a maximum recorded for an optimum water content.

In our experiments, it was observed that when the activator was added to the mixing bowl (step 3 of the mixing procedure – see section on mix preparation) and until the 2nd minute of mixing, the GPM mixes seemed very stiff. This was caused by the very high water demand (more than twice the value determined for Portland cement – see Figure 9) of the finely ground aluminosilicate precursor, which at this early stage of mixing came into contact with the lubricating liquid. However, with further mixing (sometimes between 3rd and 5th minute counting from time zero), the mixes became much more workable. By partially dissolving the solid part of the precursor, the amount of liquid to solid was increased, hence the mixes became more workable.

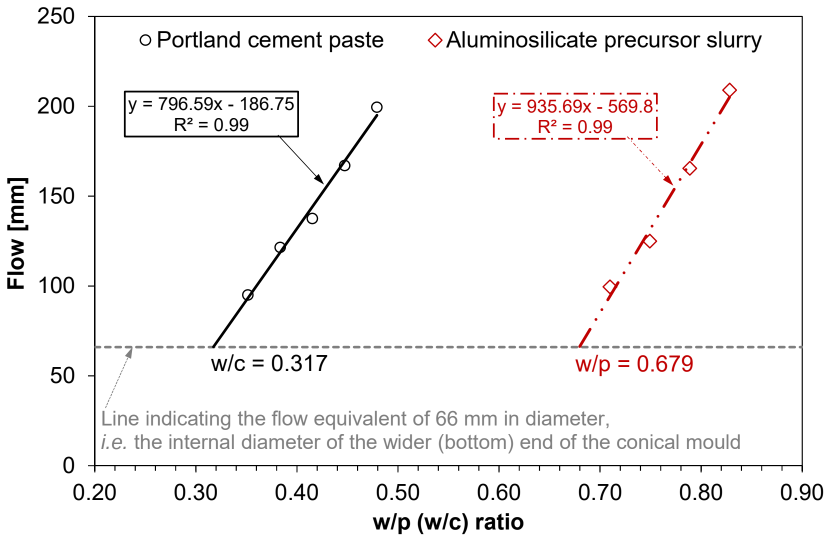

Figure 9: Water demand of the aluminosilicate precursor and Portland cement.

In our work the water content of GPM-2 mixes was kept constant, but their alkalinity (related to the content of the chemical activator), increased with the increase in paste volume – see mix proportions shown in Table 5. Therefore, based on above assumptions it can be postulated that at low w/s ratios (*i.e.* between 0.275 and 0.375), there was high alkalinity from the activator in the system, but insufficient amount of water slowed the dissolution process. At high w/s ratios (*i.e.* >0.45), there was too much water, and the alkalinity of the system was compromised, which slowed the dissolution. The optimum ratio of water-to-alkalinity, for which the dissolution rate of aluminosilicates was high, seems to be between w/s ratio of 0.375 and 0.45. As the aluminosilicate precursor had a very high water demand, the lower dissolution degree (at low and high water contents) would cause an increase in an overall surface area of solids which has to be lubricated. This in turn would negatively impact the workability of fresh geopolymer mortars. Further effort is required to understand the role of water and its content on the initial kinetics of the geopolymer reaction and the resulting implications for the workability/rheology of fresh geopolymer mix.

All of the GPM mixes presented in this paper were made with an activator of constant composition (*i.e.* water content and SiO_2/K_2O molar ratio) and a constant mass ratio of activator to aluminosilicate precursor (*i.e.* alkali dosage). It is assumed that changing these composition parameters could result in the shift of the optimal range of the w/s ratios necessary to obtain maximum workability. Since the activator is the most expensive component of the geopolymer binder, the above findings have significant practical implications on the mix design of this type of concrete. In order to provide an economic geopolymer mix proportion and obtain maximum workability, mix composition optimisation, targeting a minimum content of activator, is necessary.

The general trends for the slump and flow of both GPM-0 and GPM-1 mixes were very similar even though the workability of the GPM-0 mixes was slightly lower than that of the GPM-1 mixes (Figure 6 and Figure 7). GPM-0 mixes were made with varied paste volumes (439.5–510.4 L/m^3) while GPM-1 were with a fixed paste volume of 500 L/m^3, and thus the lower slump and flow values of GPM-0. For a given w/s ratio GPM-1 mixes showed significantly higher workability than their PCM-1 counterparts made with the same w/c ratio (all made with 500 L/m^3 of paste). Similarly, for GPM-2 mixes both the slump and flow had higher values than for the corresponding PCM-2 mixes proportioned with a constant water content. It is worth emphasising that GPM-1 and GPM-2 mixes had lower design free water contents than the corresponding PCMs (see Table 5 and Table 6). Therefore, it was possible to make highly workable GPM mixes with w/s ratios below 0.35, which is rather unachievable for Portland cement systems without the use of plasticisers or superplasticisers.

4.2.2 Setting time

Determination of the initial and final setting times is very important, because they give practitioners an indication of the time available for handling the fresh concrete (transport, placing, compaction and finishing). The effect of the w/s ratio and the paste volume variation on initial and final setting times of GPM-0 mixes, modelled using the CCD, is shown in Figure 10a and Figure 10b, respectively. Models for these two properties are shown in Table 8 and are given by Eq. 8 and Eq. 9.

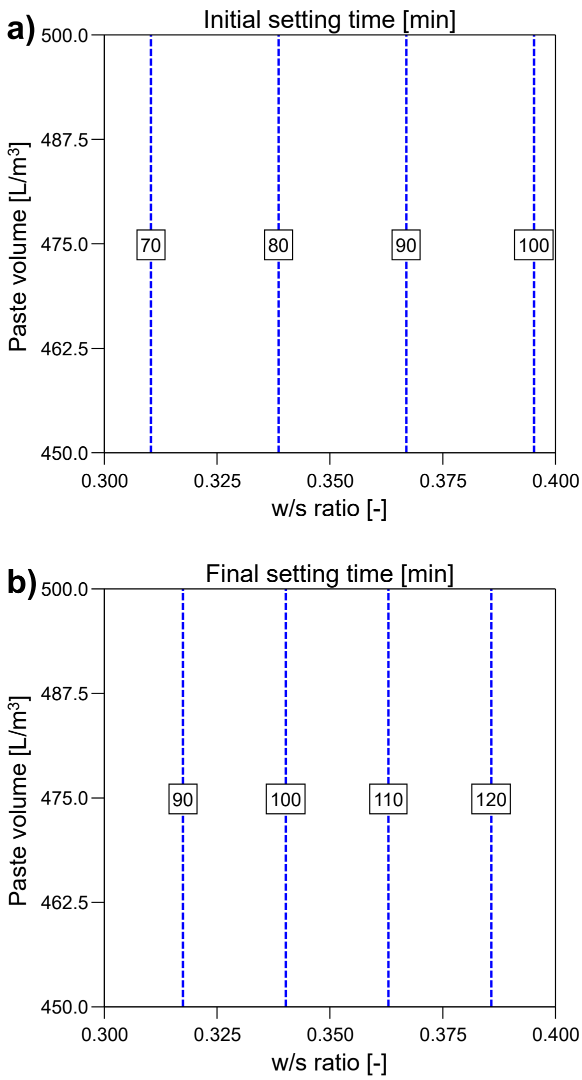

Figure 10: Contour plots developed for a) initial setting time and b) final setting time of GPM-0 mixes.

The setting times were relatively short; ranging from 46 to 117 minutes for initial set and from 59 to 145 minutes for final setting. It was found that an increase in the w/s ratio caused an increase in both properties. Neither paste volume, nor any of the higher degree effects, had a significant influence on the setting times.

As mentioned earlier, for all GPM mixes the geopolymer binder was made with an activator of constant composition and a constant mass ratio of activator to aluminosilicate precursor. Therefore, for mixes with the same paste volume, an increase in w/s ratio resulted in an increase in the free water content and a decrease in both the activator content and precursor content. Consequently, an increase was observed in the initial and finial setting times with an increase in w/s ratios resulting in a lower rate of geopolymerisation reaction (*i.e.* mainly polycondensation reaction responsible for microstructure forming [48]), caused by dilution of the chemical activator [45].

The relatively short setting times of GPM mixes were a consequence of blending the calcined lithomarge with small addition of GGBS in the aluminosilicate precursor [26]. It was reported that the addition of GGBS provides a source of calcium which facilitates reduction in setting time [48, 49]. Removal of GGBS from the blend with calcined lithomarge would still result in the geopolymer mixes setting, but the setting process would take several hours [26, 49]. Therefore, changing the content of GGBS in the aluminosilicate precursor based on the calcined lithomarge gives the advantage of controlling the setting time, hence allowing the setting characteristics to be tailored for the specific application.

The time interval between initial and final setting times decreased with a decrease in the w/s ratio (see Table 7). This may have adverse practical implications, as it gives relatively short time for finishing the surface of cast concrete.

4.2.3 Compressive strength

The effect of the w/s ratio and the paste volume on compressive strengths (at 1-, 7- and 28-day) of GPM-0 mixes, established using the CCD, is shown in Figure 11. Models for these strengths are also reported in Table 8 and are given by equations 10, 11 and 12.

It was found that the w/s ratio had the largest influence on the compressive strength at each investigated age; an increase in the w/s ratio led to a decrease in compressive strength. Effects of the paste volume and all high order effects, except for the β_{AA} effect for 7-day strength, were found to be insignificant. Similar results on the effect of w/s ratios were reported in literature [50, 51]; however, the strength of the kaolin based geopolymer concrete was mainly controlled by the intrinsic strength of the geopolymer binder (related to its chemical composition); the effect of paste volume was insignificant [50]. The negative effect of increasing w/s ratio on the compressive strength can be attributed to the increase in space occupied by water within the geopolymer matrix, resulting in increased porosity, which in turn leads to a decrease in compressive strength [51].

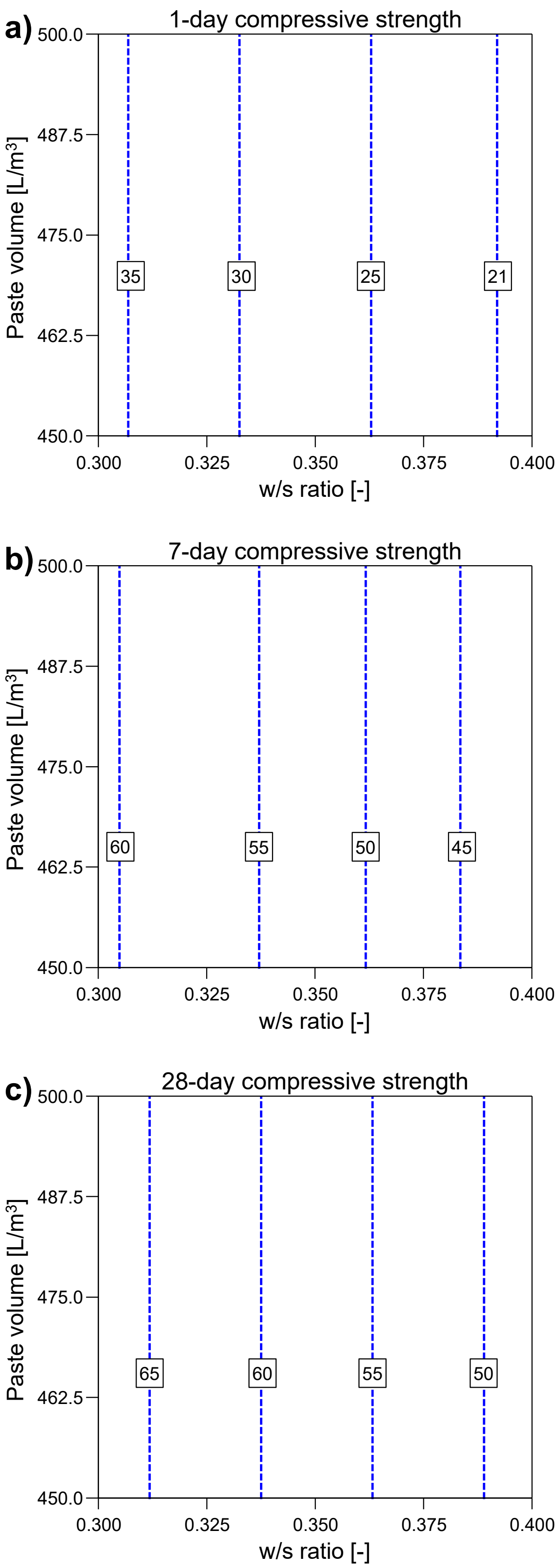

Figure 11: Contour plots developed for a) 1-day compressive strength, b) 7-day compressive strength, and c) 28-day compressive strength of GPM-0 mixes.

The 1-, 7- and 28-day compressive strengths of PCM and GPM mixes are shown in Figure 12. At each testing age, the strength of mortars made with both types of binder decreased with the increase in w/s ratio or w/c ratio, respectively.

Linear trends between w/c ratio and compressive strength were established for PCM, irrespective of testing age. The relationship between the w/s ratio and compressive strength were found to be approximately linear for GPM-0 mixes, while they were nonlinear for geopolymer mix families GPM-1 and GPM-2. The deviation from linearity in GPM-1 and GPM-2 mixes was observed at w/s ratios of above 0.4. The linear relationship established for GPM-0 was most probably the consequence of varying both w/s ratio and paste volume according to the CCD experimental plan. Nevertheless, the nature of the nonlinear behaviour of GPM mixes is unclear and requires further investigation.

Considering each investigated age (Figure 12), for given w/c ratios, the strengths of Portland cement mixes proportioned with a fixed paste volume (PCM-1) and with a fixed water content (PCM-2) were comparable. Therefore, it can be concluded that the paste volume had no effect on 1-day strength and only a minor influence at later ages. Similar assumptions can be made for geopolymer mixes, as the paste volume had only a minor effect on the compressive strength of GPM-1 and GPM-2 mixes made with the same w/s ratio.

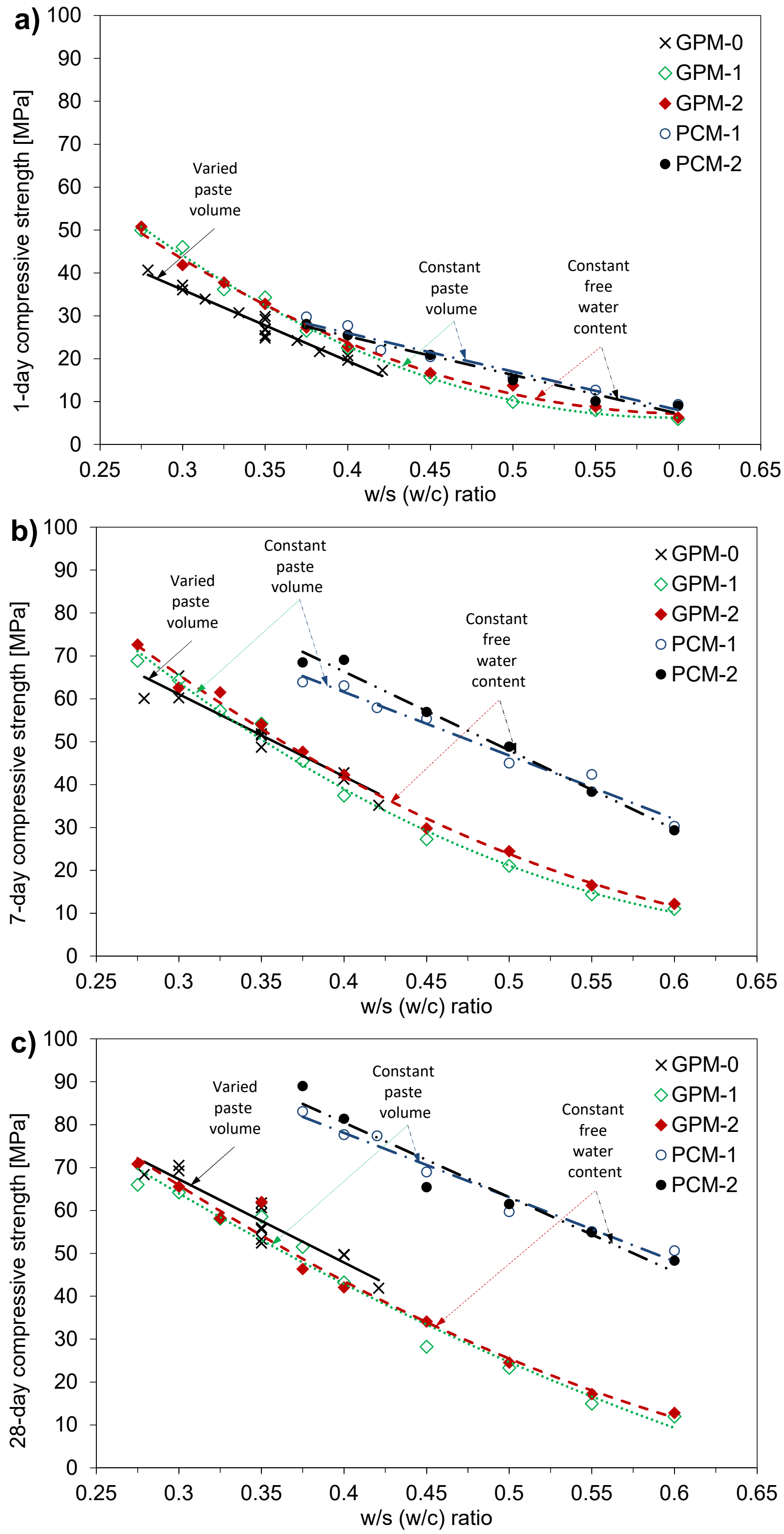

Figure 12: Influence of w/s ratio and w/c ratio on the compressive strength of GPM and PCM mixes respectively at a) 1-day, b) 7-day and c) 28-day.

It is worth noting that, irrespective of the w/s ratios used, GPMs had very high 1-day strengths when compared to the room temperature cured metakaolin mixes reported in literature [49]. Relatively high strengths resulted from blending the calcined lithomarge with a small quantity of GGBS to form the aluminosilicate precursor [26, 49].

At equivalent w/s and w/c ratios (between 0.375 and 0.6), GPMs had slightly lower or comparable 1-day compressive strengths to PCMs. At 7-days and 28-days the strength of GPMs was much lower than matching PCM mixes. GPMs gained strength up to the age of 7 days, and afterwards there was no significant increase in strength (strength at 7-day and 28-day were very similar). This indicates that the geopolymer reaction was nearly completed at this age. In contrast, due to cement hydration, PCMs gained strength up to the age of 28 days.

4.3 Direct comparison of properties for selected geopolymer and cement based mortars

To directly compare the performance of geopolymer and Portland cement mortar mixes, two formulations with the same paste volume of 500 L/m^3 were investigated for each of these two binder types (see Table 10). Considering normal and high strength applications, two characteristic strength grades were chosen: 37.5 MPa and 60 MPa. To calculate the desired target mean strength, a margin was added to the characteristic strength (see equations 13 and 14) [52]. Based on the BRE mix design guidelines [52], the following parameters for equations 13 and 14 were chosen: s = 8 MPa and k = 1.64 (for 5% defective samples), which give the margin value of 13.1 MPa.

$$f_m = f_c + M \qquad \textbf{Eq. 13}$$

$M = k \cdot s$ **Eq. 14**

where f_m is the target mean strength, [MPa], f_c is the specific characteristic strength, [MPa], M is the margin, [MPa], s is the standard deviation, [MPa], k is a constant representing a percentage of defectives, [-].

Preliminary w/s or w/c ratios were estimated based on the 28-day strength results presented in Figure 12c. The final w/s and w/c ratios were evaluated after trial mixes and along with mix proportion parameters are shown in Table 10 (reference to mix compositions already presented in Table 5 and Table 6 are also reported). Mixes were tested for workability, setting time and compressive strength. It is worth noting that, behaviour assessment and direct comparison of the resistance of these four mortar mixes to chemical attacks by sulfate and mineral acid solutions has been reported elsewhere [21].

The results for four selected mixes were reported and are summarised in Table 10:

- Workability, determined with slump and flow, was higher for mixes having high w/s or w/c ratios. Even though geopolymer mixes had very low free water contents (at least 65 L/m^3 less water than comparable PCMs) resulting in very low w/s ratios, their slump was comparable to that of PCM mixes.
- Initial and final setting times increased with the increase in w/s ratio or w/c ratio. However, geopolymer mixes showed much shorter initial and final setting times compared to those obtained for cement-based mixes. Also, time intervals between initial and final setting times were much shorter for geopolymer mixes, giving only a limited time to finish the surface.

- Geopolymer mixes showed very rapid strength gain, achieving 55–66% of their 28-day strength in the first 24 hours after mixing whilst equivalent PCMs gained only 18–28%. Therefore, at the age of 1 day, GPM-37.5 had a strength 3 times higher than PCM-37.5, while GPM-60 strength was more than double that of PCM-60. The average 28-day compressive strengths were within a maximum of 4.3 MPa (6%) of the target strength values, *i.e.* 50.6 and 73.1 MPa.

From the findings in both phases it transpires that lithomarge-based geopolymer binder can be used to proportion workable, fast setting GPM mixes cured at room temperature. A range of w/s ratios can be used to achieve a wide range of compressive strengths. Importantly, high 1-day compressive strength can be achieved using low w/s ratios.

Table 10: Properties of selected GPM and PCM mixes

Mortar binder type	Geopolymer-based		PC-based	
Characteristic strength class	**37.5 MPa**	**60 MPa**	**37.5 MPa**	**60 MPa**
Mix reference (ID of mix composition in Table 5 and Table 6)	**GPM-37.5 (GPM-1-5)**	**GPM-60 (GPM-1-1)**	**PCM-37.5 (PCM-1-7)**	**PCM-60 (PCM-1-3)**
w/s ratio	0.375	0.275	-	-
w/c ratio	-	-	0.600	0.420
Paste volume [L/m^3]	500	500	500	500
Free water content [kg/m^3]	256	218	326	284
Slump [mm]	82	12	65	17
Flow [mm]	212	106	223	162
Initial setting time [min]	78	49	323	213
Final setting time [min]	98	63	440	307
1-day compressive strength [MPa]	27.9	51.2	9.3	22.0
7-day compressive strength [MPa]	42.5	69.7	30.3	57.9
28-day compressive strength [MPa]	49.9	77.0	50.6	77.4

5 CONCLUSIONS

On the basis of the presented results, the following conclusions have been drawn:

- Statistically designed experiments (mixes GPM-0) revealed that the workability of the GPM formulated using the aluminosilicate precursor based on calcined lithomarge and verified using slump and flow tests, was governed by both w/s ratio and paste volume, but the w/s ratio had a dominant effect on this property. GPM mortars had very short initial and final setting times. Both setting times were influenced by w/s ratio only. It was found that at each investigated age, *i.e.* 1, 7 and 28 days, the w/s ratio had the only influence on decreasing the compressive strength.

- The slump and flow of GPM and PCM mortar mixes made with a constant paste volume (GPM-1 and PCM-1, respectively) increased with an increase in w/s or w/c ratio.
- GPM mixes proportioned using a constant water content (GPM-2, GPM-3 and GPM-4) showed a non-linear relationship between w/s ratio and workability. It was established that this behaviour could be associated with changes to paste/sand proportions and/or water to alkali proportions. In contrast, the workability of conventional Portland cement mixes made with a constant free water content (PCM-2) increased linearly with an increase in w/c ratio.
- Direct comparison of GPM and PCM mixes, proportioned with the same paste volume and two compressive strength classes (normal of 37.5 MPa and high of 60 MPa), showed that workable geopolymer mixes could be proportioned with at least 65 L /m^3 less free water than comparable Portland cement mixes. Geopolymer mixes had much shorter initial and final setting times than those obtained for cement-based mixes. GPMs showed very rapid compressive strength development, achieving 55–66% of their 28-day strengths within the first 24 hours after mixing. Corresponding PCMs gained only 18–28% within this time.

The results presented are very promising for designers and producers of concrete. Despite differences in established relationships, the investigated geopolymer mix proportion parameters influenced the tested properties of GPMs in a similar way as the mix proportion parameters of Portland cement systems affected the properties of PCMs. Therefore, this lithomarge-based geopolymer binder can be used to make mortars, and potentially concretes, in the same way and using the same techniques as those used for cement-based mixes. Work is continuing aiming at the development of a concrete mix design methodology for this geopolymer binder.

ACKNOWLEDGEMENTS

The work reported here was a part of an Invest Northern Ireland funded collaborative research project (Ref. No.: RDO212970 – Development and commercialisation of banahCEM geopolymer binder) between Queen's University Belfast and banah UK Ltd. The authors are grateful to the Invest Northern Ireland for the financial support and to the School of Natural and Built Environment for provided facilities.

REFERENCES

1. J.L. Provis, and S.A. Bernal, "Geopolymers and Related Alkali-Activated Materials", *Annual Review of Materials Research*, Vol. 44, 2014, pp. 299–327.
2. RILEM TC 224-AAM. Alkali-Activated Materials: State-of-the-Art Report, RILEM State-of-the-Art Reports Volume 13, Eds. J.L. Provis and J.S.J. van Deventer, 2014, Springer/RILEM, Dordrecht, 396 pp.
3. P. Duxson, J.L. Provis, G.C. Lukey and J.S.J. Van Deventer, "The role of inorganic polymer technology in the development of 'green concrete'" *Cement and Concrete Research*, Vol. 37, No. 12, 2007, pp. 1590–1597.
4. M. Granizo, M. Blanco-Varela, and A. Palomo, "Influence of the starting kaolin on alkali-activated materials based on metakaolin. Study of the reaction parameters by isothermal conduction calorimetry", *Journal of Materials Science*, Vol. 35, 2000, pp. 6309–6315.
5. Z. Zhang, H. Wang, J.L. Provis, F. Bullen, A. Reid, and Y. Zhu, "Quantitative kinetic and structural analysis of geopolymers. Part 1. The activation of metakaolin with sodium

hydroxide”, *Thermochimica Acta*, Vol. 539, 2012, pp. 23–33.

6. H. Xu, and J.S.J. van Deventer, “The geopolymerisation of alumino-silicate minerals”, *International Journal of Mineral Processing*, Vol. 59, No. 3, 2000, pp. 247–266.

7. H. Xu, and J.S.J. van Deventer, “Geopolymerisation of multiple minerals”, *Minerals Engineering*, Vol. 15, No. 12, 2002, pp. 1131–1139.

8. A. Buchwald, M. Hohmann, K. Posern, and E. Brendler, “The suitability of thermally activated illite/smectite clay as raw material for geopolymer binders”, *Applied Clay Science*, Vol. 46, No. 3, 2009, pp. 300–304.

9. H. Xu, and J.S.J. Van Deventer, “Microstructural characterisation of geopolymers synthesised from kaolinite/stilbite mixtures using XRD, MAS-NMR, SEM/EDX, TEM/EDX, and HREM”, *Cement and Concrete Research*, Vol. 32, No. 11, 2002, pp. 1705–1716.

10. T. Bakhareva, J.G. Sanjayana, and Yi-BingChengb, “Alkali activation of Australian slag cements”, *Cement and Concrete Research*”, Vol. 29, No. 1, 1999, pp. 113-120.

11. S.A. Bernal, R.San Nicolas, J.S.J. van Deventer, and J.L. Provis, “Alkali-activated slag cements produced with a blended sodium carbonate/sodium silicate activator”, *Advances in Cement Research*, Vol. 28, No. 4, 2016, pp. 262–273.

12. M. Soutsos, A.P. Boyle, R. Vinai, A. Hadjierakleous, and S.J. Barnett, “Factors influencing the compressive strength of fly ash based geopolymers”, *Construction and Building Materials*, Vol. 110, 2016, pp. 355–368.

13. H.K. Tchakoute, A. Elimbi, E. Yanne, and C.N. Djangang, “Utilization of volcanic ashes for the production of geopolymers cured at ambient temperature”, *Cement and Concrete Composites*, Vol. 38, 2013, pp. 75–81.

14. R. Rajamma, J.A. Labrincha, and V.M. Ferreira, “Alkali activation of biomass fly ash–metakaolin blends”, *Fuel*, Vol. 98, 2012, pp. 265–271.

15. R. Arellano-Aguilar, O. Burciaga-Díaz, A. Gorokhovsky, and J.I. Escalante-García,

"Geopolymer mortars based on a low grade metakaolin: Effects of the chemical composition, temperature and aggregate:binder ratio", *Construction and Building Materials*, Vol. 50, 2014, pp. 642–648.

16. A. Autef, E. Joussein, A. Poulesquen, G. Gasgnier, S. Pronier, I. Sobrados, J. Sanz, and S. Rossignol, "Influence of metakaolin purities on potassium geopolymer formulation: The existence of several networks", *Journal of Colloid and Interface Science*, Vol. 408, 2013, pp. 43–53.

17. M.A. Longhi, E.D. Rodríguez, S.A. Bernal, J.L. Provis, and A.P. Kirchheim, "Valorisation of a kaolin mining waste for the production of geopolymers", *Journal of Cleaner Production*, Vol. 115, 2016, pp. 265–272.

18. J.A. McIntosh, J. Kwasny, and M.N. Soutsos, "Evaluation of Northern Irish Laterites as Precursor Materials for Geopolymer Binders", *34th Cement and Concrete Science Conference*, Sheffield, UK, 14–17 Sep 2014, 6 p.

19. A. Mcintosh, S.E.M. Lawther, J. Kwasny, M.N. Soutsos, D. Cleland, and S. Nanukuttan, "Selection and characterisation of geological materials for use as geopolymer precursors", *Advances in Applied Ceramics*, DOI: 10.1179/1743676115Y.0000000055.

20. J. Kwasny, M.N. Soutsos, J.A. McIntosh, and D.J. Cleland, "banahCEM – comparison of properties of a laterite-based geopolymer with conventional concrete", *9th International Concrete Conference 2016. Environment, Efficiency and Economic Challenges for Concrete*, University of Dundee, Scotland, UK, 4–6 Jul 2016, pp. 383–394. Eds. M.R. Jones, M.D. Newlands, J.E. Halliday, L.J. Csetenyi, L. Zheng, M.J. McCarthy and T.D. Dyer.

21. J. Kwasny, T.A. Aiken, M.N. Soutsos, J.A. McIntosh, and D.J. Cleland, "Sulfate and acid resistance of lithomarge-based geopolymer mortars", *Construction and Building Materials*, Vol. 166, 2018, pp. 537–553.

22. V.A. Eyles, "Note on the Interbasaltic Horizon in Northern Ireland", *Quarterly Journal of*

the Geological Society, Vol. 106, 1950, pp. 136–137.

23. M.R. Cooper, “Paleogene Extrusive Igneous Rocks”, in “The Geology of Northern Ireland”, (ed. W. I. Mitchell), Belfast, N. Ireland, *GSNI*, 2004, pp. 167–178.

24. Neville, A.M., “Properties of Concrete”, 4th ed., *Longman*, Essex, UK, 1996, 844 pp.

25. D.C. Montgomery, “Design and Analysis of Experiments”, 6th ed., *John Wiley & Sons*, 2005, 643 pp.

26. J.M. Blackstock, J. Neill, and J.A. McIntosh, 2017, “Geopolymeric concrete and methods of forming it from a basaltic precursor”, European Patent, EP 2 451 758 B1.

27. British Standards Institution, “BS EN 15167-1:2006 – Ground granulated blast furnace slag for use in concrete, mortar and grout. Definitions, specifications and conformity criteria”, *BSI*, London, UK, 2006.

28. British Standards Institution, “BS EN 197-1:2011 – Cement. Composition, specifications and conformity criteria for common cements”, *BSI*, London, UK, 2011.

29. British Standards Institution, “BS 812-2:1995 – Testing aggregates. Methods for determination of density”, *BSI*, London, UK, 1995.

30. British Standards Institution, "BS 812-103.1:1985 – Testing aggregates. Method for determination of particle size distribution. Sieve tests", *BSI*, London, UK, 1985.

31. P.C. Aitcin, “High Strength Concrete (Modern Concrete Technology)”, *E & FN Spon*, London, UK, 1998, 624 pp.

32. British Standards Institution, “BS 6463-103:1999 – Quicklime, hydrated lime and natural calcium carbonate. Methods for physical testing”, *BSI*, London, UK, 1999.

33. British Standards Institution, “BS EN 12350-2:2009 – Testing fresh concrete. Slump test”, *BSI*, London, UK, 2009.

34. British Standards Institution, “BS EN 13395-1:2002 – Products and systems for the protection and repair of concrete structures. Test methods. Determination of workability. Test

for flow of thixotropic mortars", *BSI*, London, UK, 2002.

35. Domone, C. Hsi-Wen, Testing of binders for high performance concrete, *Cement and Concrete Research*, Vol. 27, No. 8, 1997, pp. 1141–1147.

36. ASTM International, "ASTM C403/C403M-08 – Standard Test Method for Time of Setting of Concrete Mixtures by Penetration Resistance", *Annual Book of ASTM Standards, ASTM International*, West Conshohocken, United States, 2009.

37. British Standards Institution, "BS EN 12390-3:2009 – Testing hardened concrete. Compressive strength of test specimens", *BSI*, London, UK, 2009.

38. Design-Expert 7.1 software for design of experiments. Stat-Ease Inc., Statistics Made Easy, USA, 2005.

39. S.S. Shapiro, and M.B. Wilk, "An analysis of variance test for normality (complete samples)", *Biometrika*, Vol. 52, No. 3 and 4, 1965, pp. 591–611.

40. G.E.P. Box, and D.R. Cox, "An analysis of transformations", *Journal of the Royal Statistical Society, Series B*, Vol. 26, 1964, pp. 211–234.

41. L.G. Li, and A.K.H. Kwan, "Mortar design based on water film thickness", *Construction and Building Materials*, Vol. 25, No. 5, 2011, pp. 2381–2390.

42. J. Kwasny, M. Sonebi, J. Plasse, and S. Amziane, "Influence of rheology on the quality of surface finish of cement-based mortars", *Construction and Building Materials*, Vol. 89, 2015, pp. 102–109.

43. de Larrard, F., "Concrete mixture proportioning: a scientific approach" E & FN Spon (Routledge), London, UK, 1999, 421 pp.

44. P. Duxson, A. Fernández-Jiménez, J.L. Provis, G.C. Lukey, A. Palomo, J.S.J. van Deventer, "Geopolymer technology: the current state of the art", *Journal of Material Science*, Vol. 42, 2007, pp. 2917–2933.

45. Z. Zuhua, Y. Xiao, Z. Huajun, C. Yue, "Role of water in the synthesis of calcined kaolin-

based geopolymer", *Applied Clay Science*, Vol. 43, No. 2, 2009, pp. 218–223.

46. X. Yao, Z. Zhang, H. Zhu, and Y. Chen, "Geopolymerization process of alkali–metakaolinite characterized by isothermal calorimetry", *Thermochimica Acta*, Vol. 493, No. 1–2, 2009, pp. 49–54.

47. H. Rahier, B. Van Mele, and J. Wastiels, "Low-temperature synthesized aluminosilicate glasses: Part II Rheological transformations during low-temperature cure and high-temperature properties of a model compound", *Journal of Materials Science*, Vol. 31, No. 1, 1996, pp. 80–85.

48. A. Buchwald, R. Tatarin, and D. Stephan, "Reaction progress of alkaline-activated metakaolin-ground granulated blast furnace slag blends", *Journal of Materials Science*, Vol. 44, No. 20, 2009, pp. 5609–5617.

49. G. Samson, M. Cyr, and X.X. Gao, "Formulation and characterization of blended alkali-activated materials based on flash-calcined metakaolin, fly ash and GGBS", *Construction and Building Materials*, Vol. 144, 2017, pp. 50–64.

50. R. Pouhet, and M. Cyr, "Formulation and performance of flash metakaolin geopolymer concretes", *Construction and Building Materials*, Vol. 120, 2016, pp. 150–160.

51. M. Steveson, and K. Sagoe-Crentsil, "Relationships between composition, structure and strength of inorganic polymers: Part I Metakaolin-derived inorganic polymers*", Journal of Materials Science,* Vol. 40, No. 8, 2005, pp. 2023–2036.

52. D.C. Teychenne, R.E. Franklin, H.C. Erntroy, "Design of normal concrete mixes: second edition", BRE Report 331, 2nd edition, *BREPress*, 1997.